

Mapping Novel and fine mapping of previously identified QTL associated with Glucose tolerance using the Collaborative Cross mice.

Hanifa J. Abu-Toamih-Atamni^{1,#}, Iqbal M. Lone^{1,#}, Ilona Binenbaum^{2,3,#}, Richard Mott⁴,
Eleftherios Pilalis⁵, Aristotelis Chatziioannou^{2,5} and Fuad A. Iraqi¹

¹Department of Clinical Microbiology and Immunology, Faculty of Medicine, Tel-Aviv University, Tel-Aviv 69978, Israel.

²Center of Systems Biology, Biomedical Research Foundation of the Academy of Athens, Soranou Ephessiou str, 11527, Athens, Greece

³Division of Pediatric Hematology-Oncology, First Department of Pediatrics, National and Kapodistrian University of Athens, Athens, Greece

⁴Department of Genetics, University College of London, UK

⁵e-NIOS Applications PC, 196 Syggrou Ave., 17671, Kallithea, Greece

#Have an equal contribution

Hanifa Abu-Toamih Atamni: hanifajalal@hotmail.com

Iqbal M. Lone: iqbalzoo84@gmail.com

Ilona Binenbaum: ilonab@med.uoa.gr

Richard Mott: r.mott@ucl.ac.uk

Eleftherios Pilalis: epilalis@e-nios.com

Aristotelis Chatziioannou: achatzi@bioacademy.gr

Fuad A. Iraqi: fuadi@tauex.tau.ac.il

Corresponding author:

Prof. Fuad A. Iraqi

Department of Clinical Microbiology and Immunology

Sackler Faculty of Medicine

Tel Aviv University, Ramat Aviv

Tel Aviv 69978

Israel

Email: fuadi@tauex.tau.ac.il

Abstract

A chronic metabolic illness, type 2 diabetes (T2D) is a polygenic and multifactorial complicated disease. With an estimated 463 million persons aged 20 to 79 having diabetes, the number is expected to rise to 700 million by 2045, creating a significant worldwide health burden. Polygenic variants of diabetes are influenced by environmental variables. T2D is regarded as a silent illness that can advance for years before being diagnosed. Finding genetic markers for T2D and metabolic syndrome in groups with similar environmental exposure is therefore essential to understanding the mechanism of such complex characteristic illnesses. So herein, we demonstrated the exclusive use of the collaborative cross (CC) mouse reference population to identify novel quantitative trait loci (QTL) and, subsequently, suggested genes associated with host glucose tolerance in response to a high-fat diet. In this study, we used 539 mice from 60 different CC lines. The diabetogenic effect in response to high-fat dietary challenge was measured by the three-hour intraperitoneal glucose tolerance test (IPGTT) test after 12 weeks of dietary challenge. Data analysis was performed using a statistical software package IBM SPSS Statistic 23. Afterward, blood glucose concentration at the specific and between different time points during the IPGTT assay and the total area under the curve (AUC0-180) of the glucose clearance was computed and utilized as a marker for the presence and severity of diabetes. The observed AUC0-180 averages for males and females were 51267.5 and 36537.5 mg/dL, respectively, representing a 1.4-fold difference in favor of females with lower AUC0-180 indicating adequate glucose clearance. The AUC0-180 mean differences between the sexes within each specific CC line varied widely within the CC population. A total of 46 QTL associated with the different studied phenotypes, designated as **T2DSL** and its number, for **Type 2 Diabetes Specific Locus** and its number, were identified during our study, among which 19 QTL were not previously mapped. The genomic interval of the remaining 27 QTL previously reported, were fine mapped in our study. The genomic positions of 40 of the mapped QTL overlapped (clustered) on 11 different peaks or close genomic positions, while the remaining 6 QTL were unique. Further, our study showed a complex pattern of haplotype effects of the founders, with the wild-derived strains (mainly PWK) playing a significant role in the increase of AUC values.

Introduction

The American Diabetes Association (ADA 2021) has classified diabetes into the following four general categories: (1) Type 1 diabetes (due to autoimmune β -cell destruction, usually leading to absolute insulin deficiency, including latent autoimmune diabetes of adulthood); (2) Type 2 diabetes (due to a progressive loss of adequate β -cell insulin secretion frequently on the background of insulin resistance); (3) specific types of diabetes due to other causes, e.g., monogenic diabetes syndromes (MGDS), such as neonatal diabetes and maturity-onset diabetes of the young, diseases of the exocrine pancreas (such as cystic fibrosis and pancreatitis), and drug- or chemical-induced diabetes (such as with glucocorticoid use, in the treatment of HIV/AIDS, or after organ transplantation); and (4) gestational diabetes mellitus (diabetes diagnosed in the second or third trimester of pregnancy that was not overt diabetes before gestation). In this study, we will focus on the genetic bases of Type 2 diabetes (T2D) that were identified by using the CC mouse model. T2D is a polygenic and multifactorial complex disease, defined as a chronic metabolic disorder (Abu Toamih-Atamni et al. 2016b, 2017, 2019; Ghnaim et al. 2023; Lone et al. 2023a). It's a primary global health concern, with an estimated 463 million adults aged 20–79 years with diabetes globally (~ 9.3% of the population in this age group), projected to increase up to 700 million by 2045 (Saeedi et al. 2019).

According to a World Health Organization report, there were 38 million deaths globally in 2012 due to NCDs. The four leading NCDs were cardiovascular diseases (17.5 million deaths), malignancies (8.2 million deaths), respiratory illnesses (4 million deaths), and diabetes (1.5 million deaths). The premature death rate from diabetes increased by 5% between 2000 and 2016, it is important to highlight (Ling et al. 2020). Diabetes is anticipated to be the 7th leading cause of death (up 2-3 spots from 2012 to 2030), while the yearly number of deaths from NCDs is continuously rising (unlike infectious diseases) and is estimated to climb from 38 million in 2012 to 52 million by 2030 (Mathers and Loncar 2006; Lone and Iraqi 2022). Globally, the prevalence of diabetes is rising steadily. Wild et al. (2004) predicted that the number of persons with diabetes worldwide would increase from 171 million in 2000 to 366 million by 2030, showing that the diabetes epidemic is growing rapidly even though the prevalence of obesity remains constant. A large portion of the rise in diabetes prevalence would occur in emerging nations, with the bulk of patients between the ages of 45 and 64. Sadly, it is predicted that up to 80% of diabetic patients

will eventually develop metabolic syndrome illnesses such as non-alcoholic fatty liver disease (NAFLD), cardiovascular diseases (CVD), dyslipidemia, kidney failure, and finally, mortality from a variety of these illnesses' sequelae (Buse et al. 2007; Ghnaim et al. 2023). A potentially progressive, severe liver disease NAFLD is linked to various metabolic disorders such as diabetes mellitus, obesity, dyslipidemia, and hypertension (Flisiak-Jackiewicz et al. 2021; Lone et al. 2023b). T2D is a part of the metabolic syndrome, first identified by the Reaven study, which also contains additional CVD risk factors such as insulin resistance and hyperinsulinemia, dyslipidemia, and high blood pressure (Reaven 1988).

It is well-recognized that both hereditary and environmental variables play a significant role in the pathogenesis of T2D, which varies significantly between populations and ethnic groups (Dagogo and Jack 2003; Samsom et al. 2016; Abdel Said et al., 2022; Yehia et al. 2023). Currently, genetic makeup is essential in predicting how the host will react to specific environmental factors, including whether or not they may cause T2D. The body of research on the interactions between the genome and the environment has revealed differences between ethnic communities at the level of genetic modification by specific environmental factors (Kaul and Ali 2016). T2D is a silent illness that can develop for years before being identified. Numerous metabolic issues are noticed once T2D is diagnosed, either as comorbidities or as side effects. So here, the question arises for the study of Quantitative Trait Loci (QTL) analysis of T2D to find the new QTLs for a better analysis of this disease. Although such studies have been carried out earlier as well, the need for further studies is a must as human genome-wide association studies (GWAS) surveys have revealed that at least 88 T2D-associated loci and 83 glycemic signatures (Mohlke and Boehnke 2015) require further studies to understand their biological roles and mechanisms in T2D. Thus, the search for novel glucose tolerance-specific QTL mapping in collaborative cross mice was undertaken to be presented in this study.

Like T2D, it is frequently believed that complex traits, including many host genes, influence the development of disorders associated with metabolic syndrome (gene-by-environment interactions). Standardized controlled investigations are challenging and nearly impossible in humans, despite the significant resources invested in studying the genetic epidemiology of diseases associated with metabolic syndrome using data from thousands of patients and matched control populations. It is thought that the emergence of one or more metabolic syndrome traits is mainly

driven by genetics, with dietary choices impacting how those genes are expressed. The study, in its next phase, deals with the genes associated with observed QTL.

Identification of obesity susceptibility variants has improved since the advent of GWAS (Sandholt et al. 2012). Unquestionably, the increase in the incidence of obesity worldwide is caused by changes in environmental factors. The persistence of significant individual variance in body weight among a community that shares the same environment, however, is one striking aspect of the "obesity pandemic" (Ramachandrappa and Farooqi 2011). Finding genetic markers for T2D and metabolic syndrome in groups with similar environmental exposure is therefore essential to understanding the mechanism of such complex characteristic illnesses. In our previous report (Abu Toamih-Atamni et al., 2017), using a cohort of CC mice, we mapped a significant female sex-dependent QTL at a genomic interval of around 2.5 Mbp, associated with a specific intraperitoneal glucose tolerance test (IPGTT) of calculated AUC0-180 trait, located on Chromosome 8 (32–34.5 Mbp), containing 51 genes). In the current report, we used extensive phenotypic data on T2D development assessment and demonstrated the exclusive use of the CC unique mouse reference population to identify new QTLs, as well as fine mapping a previously identified QTL associated with T2D, and subsequently genes associated with host glucose tolerance in response to a high-fat diet (HFD).

Materials and methods

Ethical statement

Mice were housed in the small animal facility of the Faculty of Medicine at Tel-Aviv University (TAU) according to the standard protocol approved by the animal use and care committee at TAU (approved experiment number M-12-025).

Housing and diet

Mice were housed, separately by sex and CC line on hardwood chip bedding in open-top cages, kept under 12 hours light/dark cycle (6:00 am–6:00 pm) at 21–23C, and fed with tap water and standard rodent chow diet ad libitum (TD.2018SC, Teklad Global, Harlan Inc., Madison, WI, USA; containing %Kcal from Fat 18 %, Protein 24 %, Carbohydrates 58 %), since weaning at age of 3 weeks, until start of the experiment at the age of 8 weeks. To induce the development of diabetogenic response, the mice were fed a purified experimental high-fat diet (TD 88137 Harlan

Teklad, Madison, WI, USA; containing 42 % of calories from fat and 34.1 % from carbohydrate, primarily sucrose) with their ages ranging from 8 to 20 weeks.

CC lines

All the CC lines used in this study were being developed at TAU animal facility. The CC lines developed by full-sib mating technique to exceed the current inbreeding generation; further details of the TAU CC colony are available in previous reports (Iraqi et al. 2008; 2012). In the current study, we used 539 mice from 60 CC lines (317 male and 222 female). Sex presentation was not equal for all CC lines due to breeding variations between the lines. The details of the mice used and the distribution in each sex of all the CC lines used have been presented in Supplementary Table 1.

Genotype

All CC lines were genotyped with high-density SNP markers, as previously described, and used (Yang et al. 2009; Iraqi et al. 2012; Vered et al. 2014; Levy et al. 2015; Abu Toamih-Atamni et al. 2016b, 2017, 2019). In brief, all SNPs were filtered out with heterozygous or missing genotypes in the 8 CC founders or those not in common between the arrays. The SNPs were mapped onto build the mouse genomes. The HAPPY HMM computed a descent probability distribution for each of the used SNPs.

Phenotype

The diabetogenic effect in response to the high-fat dietary challenge was measured by the intraperitoneal glucose tolerance test (IPGTT) (Montgomery et al. 2013; Leiter 2009) after 12 weeks of dietary challenge. For the IPGTT, mice were fasted for 6 h (6:00–12:00 am) with free access to water. Subsequently, fasting blood glucose (FBG) levels were determined at time 0 (BG0), and then a solution of glucose (2.5gr glucose per Kg mouse) was administered by intraperitoneal (IP) injection and blood glucose levels were monitored for 180 min (time 0, 15, 30, 60, 120, and 180 min, and designated as BG0, BG15, BG30, BG60, BG120, and BG180, respectively). Blood glucose levels were measured from the tail vein of the mice using U-RIGHT glucometer TD-4267 (TaiDoc Technology Corporation 3F, 5F, No. 127, Wungong 2nd Rd., 24888 Wugu Township, Taipei County, Taiwan). The AUC between any two-time points is calculated as (Time difference in minutes between sequential reads) *(Glucose level 1st time point + Glucose

level 2nd time point)/2). The quantitative glucose clearance ratio of the total 180 min IPGTT was calculated using the area under the curve (AUC) trapezoidal model from time zero (0) to time 180 min, as as the sum of the AUC between each two-time point, total $AUC_{0-180} = (AUC_{0-15} + AUC_{15-30} + AUC_{30-60} + AUC_{60-120} + AUC_{120-180})$ as previously described (Abu Toamih-Atamni et al., 2016a).

Statistical analysis

Data analysis was performed using a statistical software package IBM SPSS statistic 23. One-Way ANOVA was carried out for testing the significance of the variations of the AUC_{0-180} means between the different CC lines and a P value of 0.05 or less was considered significant.

QTL mapping

The HAPPY package also tests for the existence of a QTL at each locus using the estimated probabilities of descent from the founder strains to estimate the phenotypic effect attributable to each founder strain. If these effects are significantly different, then there is evidence for a QTL. Thus, for the initial stage of linkage analysis based on single trait analysis, a standard polyallelic “marker ” model will be used. This model tests whether there is an overall association between the marker and the trait by comparing after fitting the complete model, including the mean, any fixed effects such as sex and generation, and the marker alleles.

Founder’s Effect Analysis

Except for a few *de novo* mutations arising during breeding, all sequence variants segregating in the CC should also segregate in the CC founders. We tested which variants, under a QTL peak, were compatible with the pattern of action at the QTL. A variant with A alleles inside the locus L merges the eight CC founders into $A < 8$ groups according to whether they share the same allele at the variant ($A = 2$ in the case of SNPs). This merging is characterized by an $8 \times A$ merge matrix M_{sa} defined as 1 when strain s carries allele a , and 0 otherwise. The effect of this merging is tested by comparing the fit of the QTL model above with one in which the $N \times 8$ matrix X_{Lis} is replaced by the $N \times A$ matrix $Z_{ia} = S_s X_{Lis} M_{sa}$. We use the Perlegen SNP database (<http://mouse.perlegen.com/mouse/download.html>) to test sequence variants globally and the Sanger mouse genomes database (<http://www.sanger.ac.uk/resources/mouse/genomes/>) for individual genes. Within the QTLs, we classified the sequence variants according to the genome annotation as repetitive,

intergenic, upstream, downstream, UTR, intronic, or coding. We then classified variants according to whether their merge logP was greater or less than the corresponding haplotype based logP. The enrichment of variants with high logP values within each category was computed.

Gene Prioritisation and Functional Analysis

The functional interpretation and the gene and cellular pathway prioritization analysis of the QTL results exploited the mouse genome informatics (MGI) database resource (<http://www.informatics.jax.org/>), as this resource enables finer scrutiny of the functional ramifications of the reported QTLs, detailing genetic features located within the QTL genomic interval, related to glucose homeostasis/metabolism or the involved systems in type-2 diabetes, such as immune/endocrine systems. The MGI search revealed known genes, mRNAs, QTLs and many more. Each result observed at the MGI was further investigated in the literature for biological roles.

Functional pathway analysis was performed on the full gene lists extracted using MGI from the 95% CI for each mapped QTL an updated version of BioInfoMiner (Koutsandreas et al. 2016). BioInfoMiner exploits biological hierarchical vocabularies to detect and rank (prioritize) significantly altered processes, as well as the respective hub linker genes orchestrating the interaction of these significantly altered processes. For our analysis we utilised Gene Ontology (GO) (Ashburner et al. 2000), Reactome (Gillespie et al., 2022) and MGI Mammalian Phenotype Ontology (Smith et al. 2012). BioInfoMiner constructs an unsupervised genomic network from the significant semantic terms derived from the enrichment analysis of the input gene list, utilizing the respective ontologies. This network, in the form of a hierarchical tree in which each term is associated with various genes (bi-partite graph), is delineated after the results (ontological terms) of the initial enrichment analysis are statistically corrected through bootstrapping to eradicate annotation bias, and then clustered automatically, through the use of proper semantic similarity operators like Resnik, Lin, Jiang and Conrath etc (<https://funsimmat.bioinf.mpi-inf.mpg.de/help3.php>). The new bi-partite graph thus derived prioritizes the genes based on topological properties like the centrality of their connectivity with the functional nodes of the corrected graph, minimising the semantic annotation bias and allowing the non-trivial prioritization of critical hubs according to the architecture of the dynamic network expressing systemically the phenotype studied. In this way, systemic interpretation of complex cellular mechanisms emerging from the input gene lists

is accomplished, unearthing a vector of ranked regulatory genes with pivotal functional roles in the manifestation of the studied phenotype. The novel BioInfoMiner platform is available online at <https://bim3.e-nios.com>.

Results

An intraperitoneal glucose tolerance test (IPGTT) for 180 minutes was used to determine the diabetogenic response of the CC lines after 12 weeks of the HFD challenge. Afterward, the total area under the curve (AUC₀₋₁₈₀) of the glucose clearance was computed and utilized as a marker for the presence of diabetes; higher values of AUC₀₋₁₈₀ were linked to slower glucose clearance and even decreased glucose tolerance. Using the HAPPY software, the genotypic information of the CC lines was examined for genetic linkage with the trait AUC₀₋₁₈₀ for the entire population and then for females and males separately. The findings, including phenotypic data, QTL analysis, founder's effect analysis, and candidate gene identification, are shown below.

Significant glucose tolerance variation between CC lines

Figures 1A-C illustrate the significant differences in AUC₀₋₁₈₀ means between the entire (overall) CC lines population (Figure 1A), as well as for females and males as shown in Figure 1B and Figure 1C respectively separately. The mean AUC₀₋₁₈₀ for the entire population of CC lines (n = 539/60 CC lines) was 46484±1846 mg/dL*min, with the mean values ranging from IL-86 (representing the lowest value of 22,792 mg/dL*min) to IL-2452 (representing the highest value of 82,575, mg/dL*min). Figure 1D shows the profiles of entire assessed phenotypes in our CC mouse lines.

Male AUC₀₋₁₈₀ is significantly higher than females.

45 of the 60 total assessed CC lines (Females: 222; Males: 317) had representation from both sexes. The relevance of the combinatorial effects of sex and line interaction impacting the variance in AUC₀₋₁₈₀ means was evaluated using a two-way ANOVA. The results of the ANOVA showed that there were very significant independent sex and line effects (P<0.001) and significant Sex * Line interactions (P<0.05) that affected the variation of averages in the AUC₀₋₁₈₀ range. The observed AUC₀₋₁₈₀ averages for males and females were 51267.5 and 36537.5 mg/dL, respectively, representing a *1.4-fold difference in favor of females (lower AUC₀₋₁₈₀ indicates

effective glucose clearance). The AUC0-180 mean differences between the sexes within each specific CC line varied widely within the CC population.

Identification of candidate genes within the mapped QTL intervals

A total of 46 QTLs were identified in our study were designated as **T2DSL, for Type 2 Diabetes Specific Locus** and its **number**. These mapped QTL, along with their genomic interval locations, peak interval sizes, chromosome specificity, and specific trait, were listed in Tables 1-3, and Figures 2A-C, respectively, representing the overall population and males and females separately. 19 QTLs of the total were not previously mapped. The genomic interval of the remaining 27 QTL previously reported, their genomic intervals were fine-mapped in our study, as shown in Table 4. The genomic positions of 40 of the mapped QTL overlapped (clustered) on 11 different peaks or close genomic positions, as shown in Table 5, while the remaining 6 QTL were unique.

Mapping new QTL

Our results showed that 19 new QTLs of the whole mapped QTLs were not previously mapped in previous reports that associated with our phenotypic data. The genomic interval positions of 13 of these QTLs overlapped with previously mapped QTL (Table 4), while six of them are unique QTLs. The first new QTL T2DSL2 mapped during our study was on chromosome 2 at a position of 12.17-19.25 Mbp, peaking at 15.64 Mbp in the overall population fasting glucose condition. The other observed new QTLs of blood glucose (BG)-T180 in the overall population were T2DSL4, T2DSL5, and T2DSL7, respectively, on interval positions of 77.95-81.22, 83.94-89.71, and 89.05-92.58 Mbp with their respective peak positions at 79.26, 86.64 and 90.78 Mbp. The former QTLs, T2DSL4 and T2DSL5, were mapped on chromosome 14, while the T2DSL7 was identified on chromosome 17. In AUC0-120 phenotype in the overall population, a new QTL T2DSL9 was identified on chromosome 8 with the interval position of 125.71-132.88 Mbp, reaching its peak at 130.18 Mbp.

The major mapped QTLs were from the male population. Here in males on chromosome 2 in fasting glucose condition, a new QTL T2DSL12 was identified with an interval position of 11.54-19.02 Mbp with its peak at 15.53 Mbp. In BG-T60 a new QTL T2DSL13 on chromosome 9 with the interval position of 7.14-11.46 Mbp having its peak at 9.09 Mbp was identified. With BG-T120 phenotype a new 1 QTL T2DSL16 with the interval position of 5.94-12.30 Mbp peaked at

9.09 Mbp was identified on chromosome 9. With BG-T180 phenotype, four novel QTL T2DSL18, T2DSL19, T2DSL21, and T2DSL22 with their respective interval positions of 83.75-91.22, 77.98-82.70, 6.38-14.23 and 2.23-10.34 Mbp were identified on chromosome 7, 8, 10 and 11 respectively.

In males with phenotype AUC0-180 ,a new QTL T2DSL24 was identified on chromosome 9 with the interval position of 6.77-11.48 Mbp reaching its peak at 9.09 Mbp. In males AUC0-120 phenotype, a new QTL T2DSL30 was identified on chromosome 19 with the interval position of 60.62-62.82 Mbp, reaching its peak at 61.80 Mbp. One more new QTL T2DSL32 was identified on chromosome 9 with the interval position of 7.41-11.47 Mbp, reaching its peak at 9.09 Mbp in AUC30-60. In AUC60-120 a new QTL T2DSL33 was identified on chromosome 9 with the interval position of 6.99-11.85 Mbp. Three more new QTL T2DSL36, T2DSL39 and T2DSL42, with their respective interval positions of 7.83-14.28, 77.98-82.24, and 74.20-84.33 Mbp, were identified on chromosomes 9, 14 and X respectively. There was no novel QTL identified in any condition in the female population in our study.

Fine mapping of previously identified QTL

The other 27 QTLs observed during our study were also new but had already been identified by earlier researchers, although our study fine-mapped their interval position. In the overall population, six fine-mapped QTLs were T2DSL1, T2DSL3, T2DSL6, T2DSL8, T2DSL10, and T2DSL11 on chromosomes 8, 11, and X (Table 2). Similarly, in males, only group seventeen fine mapped QTL were observed on ten different chromosomes throughout the genome (Table 2). In the only female population, four fine-mapped QTLs observed were T2DSL43, T2DSL44, T2DSL45, and T2DSL46 on chromosomes 1, 8, and 9 (Table 2).

As far as the genome-wide significance threshold is concerned, three sets of QTL were identified during our entire study (Figure 2A-C). The first group is the one which had a 50% of genome-wide significance threshold (T2DSL13, T2DSL16, T2DSL18, T2DSL22, T2DSL25, T2DSL32, T2DSL33, T2DSL37, T2DSL41, T2DSL42, T2DSL44, and T2DSL46). The second group is formed of 14 QTL having a 90% of genome-wide significance threshold (T2DSL7, T2DSL10, T2DSL11, T2DSL15, T2DSL20, T2DSL21, T2DSL23, T2DSL27, T2DSL30, T2DSL31, T2DSL34, T2DSL40, T2DSL43, and T2DSL45). The third group is consisting of 20 QTL having a 95% of genome-wide significance threshold (T2DSL1, T2DSL2, T2DSL3, T2DSL4, T2DSL5,

T2DSL6, T2DSL8, T2DSL9, T2DSL12, T2DSL14, T2DSL17, T2DSL19, T2DSL24, T2DSL26, T2DSL28, T2DSL29, T2DSL35, T2DSL36, T2DSL38 and T2DSL39).

Overall population

These results have been presented in Table 1 and Figure 2A. The 2 reported QTL in fasting glucose condition (T2DSL1, T2DSL2) on chromosome X and chromosome 2 respectively contain 16 genes (including protein-coding genes and other genetic features (non-coding RNA/heritable phenotypic markers/gene segments/pseudogenes)) in the 50% CI and 352 in the 95% CI. Functional analysis showed these include prioritized genes involved in the regulation of the cell size and metabolic processes, such as ATP metabolic process (Ogt, Pgk1, Atp7a). Ogt (O-linked N-acetylglucosamine (GlcNAc) transferase) is one of the highly prioritized genes and is known to be involved in glycolysis regulation and insulin resistance (Yi et al. 2012).

In blood glucose (BG-T180) the 5 reported QTL (T2DSL3-T2DSL7) on four different chromosomes (Ch8, Ch14, Ch11, Ch17) contain 65 genes in the 50% CI and 434 in the 95% CI, 5 QTL. Among these genes, one necessary enriched systemic process was thyroid hormone levels regulation (with prioritized genes *Thra*, *Med1*) and a highly prioritized gene was *Pdk2* (Pyruvate Dehydrogenase Kinase 2), a protein involved in glycolysis, carbohydrate oxidation regulation, and secretome regulation. An important additional prioritized gene is *Fa2h* (fatty acid 2-hydroxylase) involved in fatty acid biosynthesis.

The two QTLs (T2DSL8, T2DSL9) reported in AUC0-120 on chromosome 8 contain 2 genes in the 50% CI and 75 in the 95% CI. Prioritized genes include *Itgb1* (integrin beta 1) and *Nrp1* (neuropilin 1) involved in cell growth regulation, and *Got2* (mitochondrial glutamic-oxaloacetic transaminase 2) an enzyme that plays a role in amino acid metabolism and the urea and tricarboxylic acid cycles. Integrin beta 1 has been found to be a crucial regulator of pancreatic β -cell expansion (Diaferia et al. 2013).

In AUC120-180 the two reported QTL (T2DSL10, T2DSL11) on chromosome 8 and chromosome 11 respectively contain 32 genes in the 50% CI and 255 in the 95% CI. There is an overlap with the above-mentioned prioritized genes for blood glucose level at T=180 including *Thra*, *Med1*, and *Fa2h*.

Males only

The results of the male population have been presented in Table 2 and Figure 2B. For the fasting glucose condition, the reported QTL (T2DSL12) on chromosome 2 contains 6 genes in the 50% CI and 107 in the 95% CI. Of interest are the interleukin receptors *Il2ra* and *Il15ra*, which belong to the “Interleukin-2 family signaling” systemic process. Both receptors have been associated with autoimmune T1D (Bobbala et al. 2017; Garg et al. 2012), and additionally SNPs in human *IL15RA* have been described which correlate with metabolic syndrome markers (Quinn and Anderson 2011).

In BG-T60 the 2 reported QTL (T2DSL13, T2DSL14) on chromosome 9 and chromosome 11 respectively contain 21 genes in the 50% CI and 126 in the 95% CI. These are highly enriched in genes involved in the systemic process “regulation of biosynthetic process, positive regulation of metabolic process & regulation of gene expression”, which involves matrix metalloproteinases (*Mmp8*, *Mmp12*), progesterone receptor (*Pgr*), gastric inhibitory polypeptide (*Gip*), *Nfe2l1*, prohibitin (*Phb*), yes-associated protein 1 (*Yap1*) and pyruvate dehydrogenase kinase 2 (*Pdk2*), which was also prioritized in the overall population analysis. Another enriched systemic process of interest was proteolysis, because of a cluster of matrix metalloproteinases genes (*Mmp13*, *Mmp8*, *Mmp12*, *Mmp1a*, *Mmp20*, *Mmp10*, *Mmp7*, *Mmp3*).

In BG-T120 the 3 reported QTL (T2DSL15-T2DSL17) on chromosome 9, chromosome 11 and chromosome 18 respectively contain 40 genes in the 50% CI and 318 in the 95% CI. The two QTL on chromosomes 9 and 11 share a significant overlap with BG-T60, and similar genes are prioritized such as matrix metalloproteinases, *Pgr*, *Phb*, *Yap1*. Some new genes that are highlighted in this set, are *Kat7* (lysine acetyltransferase 7), *Npc1* (NPC intracellular cholesterol transporter 1) and microRNAs *Mir-1* and *Mir133a*, which are all mapped to the high-level systemic process “Negative regulation of metabolic process”.

In BG-T180 the 6 reported QTL (T2DSL18-T2DSL23) on chromosomes 14, 8, 9 and chromosome 11 contain 74 genes in the 50% CI and 524 in the 95% CI. There is again significant overlap within the chromosome 9 and 11 QTL genes with *Pgr* and *Yap1* prioritized, however prioritized genes uniquely identified in this condition are caspases *Casp1*, *Casp4* and *Casp12*, and retinoic acid receptor alpha (*Rara*). The function of caspases at this time point, as key mediators of the inflammatory process, is of great interest and they have been thoroughly studied as therapeutic targets in metabolic disease. Caspase-1 inhibition, in HFD-fed obese-diabetic *LDLR^{-/-}* Leiden

mice, reduced adipose tissue inflammation, prevented development of NASH and attenuated progression of insulin resistance (Wilson and Kumar 2018). *Rara* is a key regulator of lipid/glucose metabolism, inflammation, and insulin sensitivity. *RORα^{sg/sg}* mice, a natural strain with loss of expression of the *Rara* gene, are protected against diet-induced obesity, inflammation, and insulin resistance and antagonist of *RARA* have potential beneficial effects in the management of obesity and insulin resistance (Jetten et al. 2013).

The five QTL (T2DSL24-T2DSL28) reported in AUC0-180 on chromosomes 9, 11, 5, and 18 contain 56 genes in the 50% CI and 325 in the 95% CI. In the matter of prioritized genes, there is again a significant overlap of genes from the QTLs on chromosomes 9, 11 and 18, including *Mmps*, *Yap1*, *Pgr*, *Npc*, *Nfe2l1*, *Mir-1* and *Mir133a*. An interesting gene prioritized in this phenotype analysis was *Osbp17* (oxysterol binding protein-like 7), a protein involved in sterol transport and the cellular response to cholesterol.

In AUC0-120, three QTL (T2DSL29-T2DSL31) were reported on chromosomes 11, 1, and 8 containing 15 genes in the 50% CI and 192 in the 95% CI. Homeobox genes (*Hoxb2*, *Hoxb1*, *Hoxb3*, *Hoxb8*, *Hoxb9*, *Hoxb7*, *Hoxb5*, *Hoxb13*, *Hoxb6*, *Hoxb4*) dominate the gene prioritization list, along with genes from previously analyzed phenotypes such as *Nfe2l1* and *Gip*. *Cnot1* (CCR4-NOT transcription complex, subunit 1) is a gene uniquely prioritized in this phenotype, a transcription factor important for pancreatic development both in mice and humans (De Franco et al. 2019).

In AUC30-60 the reported QTL (T2DSL32) on chromosome 9 contains 4 genes in the 50% CI and 42 in the 95% CI. Gene prioritization analysis results included *Mmps*, *Yap1* and *Pgr* and additionally highlighted *Birc2* and *Birc3* baculoviral inhibitor genes, which are involved in pancreatic beta cell stress response and are important in glucose homeostasis (Tan et al. 2013).

In AUC60-120, three QTL (T2DSL33-T2DSL35) on chromosomes 9, 5, and 18 were reported containing 25 genes in the 50% CI and 194 in the 95% CI. Again, there is significant overlap with many *Mmps* in the prioritized genes list, *Yap1*, *Birc 2* and *Birc3*, *Pgr*, *Mir-1* and *Mir133a*, and *Npc1*.

In AUC120-180 the seven reported QTL (T2DSL36-T2DSL42) on chromosomes 9, 11, 14, 18, 19 and chromosome X contain 91 genes in the 50% CI and 586 in the 95% CI. In this phenotype, two

new QTL, without overlap with the previously analyzed phenotypes, on chromosomes 19 and X, come into play. Interestingly, at this stage, the systemic process of “regulation of macroautophagy” comes into play, with *Ikbkg* (inhibitor of kappaB kinase gamma) identified as a unique prioritized gene. Other unique genes for this phenotype are *Flna* (filamin, alpha), *Atm* (ataxia telangiectasia mutated), *G6pdx* (glucose-6-phosphate dehydrogenase X-linked), and *Drd2* (dopamine receptor D2). Filamin A is known to interact with the insulin receptor and possibly has a negative role in transcriptional activation in response to insulin (He et al. 2003). A germline mutation in the *ATM* gene is known to be responsible for the recessive disorder ataxia telangiectasia (A-T) in humans, patients with A-T show marked insulin resistance and present with diabetes as a common comorbidity (Donath et al. 2020). *Atm*-deficient mice exhibit glucose intolerance, insulin resistance and impaired insulin secretion (Miles et al. 2007). Different SNPs in the *ATM* gene locus have been associated with impaired response to metformin, as well as with reduced risk of T2D (Ding et al. 2017; Harries et al. 2011). In a study with *G6pdx*^{-/-} mice, G6PD deficiency did not seem to affect glucose tolerance, however, it significantly decreased weight gain and hyperinsulinemia, suggesting a possible protective effect (Hecker et al. 2012). Finally, in *Drd*^{-/-} mice disruption of the dopamine receptor D2 has been shown to impair insulin secretion and cause glucose intolerance (García-Tornadú et al. 2010). In humans, genetic polymorphisms in the *DND* locus have been associated with susceptibility to T2D (Guigas et al. 2014) and bromocriptine, a sympatholytic D2-dopamine agonist, has been approved for the treatment of T2D (reviewed in Valiquette 2011)

Females only

These results of the female population have been presented in Table 3 and Figure 3C. For the fasting glucose condition, the reported QTL (T2DSL43) on chromosome 9 contains 38 genes in the 50% CI and 126 in the 95% CI. This locus is enriched with genes related to lipid localization, homeostasis, and metabolism based on GO annotation. Most notably the highest prioritized genes were several apolipoprotein genes (*Apoa5*, *Apoa1*, *Apoa4*, *Apoc3*). Additionally, a highly enriched MGI systemic process was “abnormal glucose homeostasis and abnormal circulating leptin level” with 8 different genes involved (*Mpzl3*, *Slc37a4*, *Cbl*, *Sidt2*, *Sc5d* (sterol-C5-desaturase), *Apoc3*, *Sik3*, *Apoa4*, *C1qtnf5*). Interestingly, *Sik3* (SIK family kinase 3) and *Cbl* (Casitas B-lineage lymphoma) are additionally associated with decreased brown adipose tissue.

In AUC0-120 the reported two QTLs on chromosome 8 (T2DSL44, T2DSL45) contain 56 genes in the 50% CI and 389 in the 95% CI. These genes include several carboxylesterases (Ces1h, Ces1c, Ces1b, Ces1e, Ces1g, Ces1f, Ces1a, Ces5a, Ces1d) which according to GO are involved in lipid metabolic processes and metallothioneins (Mt1, Mt2, Mt3, Mt3), which are involved in the response to metal ions and nitric oxide. Carboxylesterases have been widely associated with lipid metabolism and metabolic disorders and pose potential targets for the treatment of a number of human metabolic disorders (Lian et al. 2018). Metallothioneins have high antioxidant capacity and potentially can mediate the oxidative stress related with diet induced metabolic disorders. In humans, MT SNPs, particularly those in *MT1A* and *MT2A* genes, have been associated with susceptibility to metabolic diseases including diabetes (Yang et al. 2008). Additionally, the *Fto* (fat mass and obesity associated) gene is prioritized highly and associated with abnormal fat cell morphology, other prioritized genes that belong to the same systemic process are: *Irx3* (Iroquois related homeobox 3), *Ces1g*, *Arv1* (ARV1 homolog, fatty acid homeostasis modulator), *Agt* (angiotensinogen), and *Ces1d*.

Finally, in AUC0-60 the reported QTL (T2DSL46) on chromosome 1 contains 21 genes in the 50% CI and 83 in the 95% CI. These contain prioritized genes involved in systemic processes “glycosylation & carbohydrate derivative metabolic process” (*Sphk1*, *Galk1* (galactokinase 1), *Mgat5b* (mannoside acetylglucosaminyltransferase 5, isoenzyme B), *St6galnac1* and *St6galnac2* (ST6 N-Acetylgalactosaminide Alpha-2,6-Sialyltransferase 1 and 2)). and “fatty acid derivative metabolic process, cellular lipid metabolic process, small molecule metabolic process and membrane lipid metabolic process” (*Sphk1*, *Galk1*, *Acox1*, *Galr2*, *St6galnac1*).

Additional protein coding genes with relevance to glucose tolerance were related to immune system, endocrine system, and regulation of glucose homeostasis. With most relevance to the glucose homeostasis traits, we might suggest genes involved in regulation glucose homeostasis, such as *Mboat4* (MGI:2685017), named membrane-bound O-acyltransferase domain containing 4, which encodes enzymes that transfer organic acids, typically fatty acids, onto hydroxyl groups of membrane-embedded targets.

MBOAT4 mediates the octanoylation of the stomach hormone ghrelin (GOAT— Ghrelin O-Acyltransferase), which plays endocrine role in the regulation of glucose homeostasis. Another major candidate gene is *Leprotr11* (MGI:1915442), named leptin receptor overlapping transcript-

like 1, plays a role in the control of hepatic growth hormone (GH) resistance to involved between nutritional signals and GH actions on body growth and metabolism. LEPROTL1 expression is regulated in the mouse liver by physiologic and pathologic changes in glucose homeostasis. As well, we observed the Wrn gene (MGI:109635), named Werner syndrome homolog (human) and involved in age-related osteoporosis, adipose tissues/cardiovascular system/digestive/growth/size/body/ immune system/mortality/aging. Furthermore, MGI search revealed candidate genes were involved in the immune system and might be indirectly related to the T2D progress as an inflammatory disease. One of the observed genes was the Gsr gene, named glutathione reductase (MGI:95804), which had been shown to be involved in the immune response against bacterial challenge (phagocytes), catalyzed the reduction of glutathione disulfide to glutathione, alongside additional functionaries in Cardiovascular System/vision eye, also crucial for limiting tissue damage which are highly engaged to T2D metabolic syndrome health complication. Saraf gene (MGI:1915137), named store-operated calcium entry-associated regulatory factor, was involved inter alia in the Endocrine system, rather in the Pancreas development, the major organ of the body that responds to glucose levels and plays main role in glucose homeostasis. In addition to protein-coding genes, different QTL feature types were exposed, located within our QTL genomic interval having relevance to our phenotypes and therefore find mention.

Founder effect

The results of the founder effect analysis of the mapped QTLs were presented in Figures 3-5 for the overall population, only males and only females, respectively. We evaluated the effect of each founder genotype on the overall population, males and females mapped QTL interval of the assessed phenotypes. The mapped loci showed a complex pattern of haplotype effects of the founders, with the wild-derived strains (mainly PWK) playing a significant role in the increase of the different assessed AUC values except in female fasting glucose condition where NOD plays the same role instead, while NZO and NOD genotype reduces this assessed trait, although other strains also contributed (positive or negative) to the overall QTL effects.

Discussion

In our study, a total of 46 new QTLs were identified, which were thoroughly searched in literature among which 19 QTLs associated with defined traits were observed and found not to be reported,

previously. Their interval locations did not match with any other previously identified QTLs. In addition, 27 more QTLs were observed during our study but were observed earlier by different studies. In our we have fine-mapped the genomic interval positions of the previously identified QTLs. The QTL T2DSL1 which was previously identified by Smith et al. (2002) with an interval position of 98.05-160.60 Mbp has now been fine mapped by our study to an interval position of 98.61-108.30 Mbp on chromosome X. A group of seven QTL on chromosome 8 named as T2DSL3, T2DSL8, T2DSL10, T2DSL20, T2DSL31, T2DSL44 and T2DSL45, which were previously identified by Shike et al. (2001) have been finely mapped by our study. Similarly, a group of eight QTL on chromosome 11 named as T2DSL6, T2DSL11, T2DSL14, T2DSL15, T2DSL23, T2DSL26, T2DSL29 and T2DSL38 fine mapped by our study were previously identified by Allan et al. (2005). Furthermore, a group of four QTLs on chromosome 18 named as T2DSL17, T2DSL28, T2DSL35, and T2DSL40 fine mapped by our study were previously identified by Leiter et al. (1998). In addition, a group of three QTLs on chromosome 9 named T2DSL25, T2DSL37, and T2DSL43 fine mapped by our work were previously identified by Toye et al. (2005). Two QTLs on chromosome 5 named T2DSL27 and T2DSL34 fine mapped by us, were previously identified by Collin et al. (2005). In addition, a QTL on chromosome 1 previously identified by Hirayama et al. (1999) has now been fine-mapped by our research. A single QTL on chromosome 19 previously identified by Stoehr et al. (2000) with an interval position of 36.96-59.52 Mbp has now been fine-mapped by our study to an interval position of 49.05-51.16 Mbp and named as T2DSL41. The details of all the QTL fine mapped by our study have been provided in Table 4, and the overlapping of the genomic intervals have been shown in Table 5, along with their linkage groups on each chromosome indicated by chromosome location.

This paper presents the implementation of a unique CC mouse model to study the complex genetic architecture of T2D in response to the environmental dietary challenge of an HFD (42%). Accumulating data from T2D studies have repeatedly demonstrated the complexity of disease etiology, once attributed primarily to environmental risk factors and now to many genetic environments known to be controlled by interactions. Therefore, great efforts have been made to dissect the genetic architecture of T2D. This will curb alarming predictions about the T2D epidemic, first at the level of rapid diagnosis using genetic biomarkers and then at the level of personalized medicine. Achieving the challenge will require a great deal of effort, collaboration between scientists and clinicians, and a recognition that the complications of type 2 diabetes differ

from population to population and need to be classified based on genetic and environmental factors.

To date, human GWAS surveys have revealed at least several T2D-associated loci and glycaemic signatures (Mohlke and Boehnke 2015), which require further studies to understand their biological roles and mechanisms in T2D. Interestingly, none of the genes that were mapped within our QTL interval were found in the human-mapped genes. This means that our results are novel, as we've identified new genes associated with the tested trait. Recent human GWAS have had some success in identifying phenotype-genotype associations. However, these studies have several limitations, mainly due to the lack of proper control and constraints on further trials in human populations. Therefore, animal models were favoured for human disease studies to overcome these limitations.

Especially for GWAS studies, mouse models are favoured by many advantages, including the availability of mouse genomic data resources, the availability of genetic experimental tools, ease of breeding, and the ability to provide tightly controlled environmental conditions, widely used with remarkable potential (Cox and Kirche 2011; Lone et al. 2023c). To this end, CC mouse populations representing models of heterogeneous human populations were determined to analyse phenotypic-genotypic associations and highlight inter-population differences regarding shared environmental exposures. In the present study, CC lines corresponded to heterogeneous populations, HFD - 42% fat corresponded to T2D risk of environmental exposure, and QTL mapping to diabetic phenotypes (glucose intolerance, glucose tolerance) disability, measured as AUC0-180 and genotypic components.

Once the QTL has been mapped, the following steps are candidate gene search, candidate gene validation, translation of functional signaling pathways to high-level human genetics, and extensive use by basic and clinical researchers. It will be a lot of effort invested by the collaboration. In the current study, QTL mapping reveals a novel sex-specific locus representing the total area under the curve in response to HFD, calculated for the area under the curve between different time points of the IPGTT. Finally, data processing revealed distinct patterns of glucose clearance processes that differed significantly between CC lines in response to the same environmental conditions. Moreover, there was a significant sex-related effect in the entire

population of CC strains, with AUC0-180 in males higher than AUC0-180 in females, suggesting a greater impairment of glucose clearance in response to HFD in males.

Gender differences were significant as an overall trend but varied between CC strains when examined within each CC strain. Pooling analysis provides higher resolution of QTL peak positions was allowed; then Mouse Genome Informatics (MGI; <http://www.informatics.jax.org>), an international database resource for laboratory mice, was used to scan the observation intervals for candidate genes. Among the protein-encoding genes, *Mboat4* (MGI: 2685017) and *Leptol1* (MGI: 1915442) have been reported to be significantly involved in regulating glucose homeostasis and have been shown to have positive effects on AUC0-180 and glucose tolerance. In our previous report (Abu Toamih-Atamni et al., 2017), using a cohort of CC mice, we mapped a significant female sex-dependent QTL at a genomic interval of around 2.5 Mbp, associated with a specific intraperitoneal glucose tolerance test (IPGTT) of calculated AUC0-180 trait, located on Chromosome 8 (32–34.5 Mbp), containing 51 genes). Gene search located within the mapped QTL genomic intervals revealed body weight/size, genes involved in the immune system, and two main protein-coding genes involved in Glucose homeostasis, *Mboat4* and *Leptol1*. In humans, ghrelin-O-acyltransferase (GOAT), the protein encoded by the *MBOAT4* gene, mediates the physiological functions of ghrelin and modulators of GOAT have been suggested as a probable therapy for countering obesity and T2D (Khatib et al. 2015). Merge analysis highlighted the *Adrb3* (adrenergic receptor, beta 3) gene in female mice which is involved in the systemic process of diet-induced thermogenesis. The human beta3-adrenergic receptor gene (*ADRB3*) has been long investigated as a candidate gene for diabetes, and missense mutations in *ADRB3* has been shown to increase risk for type 2 diabetes (Walston et al. 1995; Lehman et al. 2006). This evidence supports the importance of phenotype associations.

PGK1 (phosphoglycerate kinase 1) is a key glycolytic enzyme and evidence suggests that activating *PGK1* enhances glucose metabolism. It has been recently proposed that *Alfuzosin* ameliorates diabetes by boosting *PGK1* activity in diabetic mice (Zhou et al. 2023). Copper transporter *ATP7A* (ATPase, Cu⁺⁺ transporting, alpha polypeptide) expression is impaired in diabetic mice, while it has been shown to have a protective function against endothelial dysfunction in T1D and restoring copper transporter function is an essential therapeutic approach for oxidant stress-dependent vascular and metabolic diseases (Sudhahar et al. 2013). Interestingly

it has been suggested that ATP7A can be exercise induced, suggesting a potential mechanism through which exercise can benefit individuals with T2D (Abdelsaid et al. 2022).

In BGT180 for the overall population, thyroid hormone regulation appears to be an important systemic process involving *Thra* and *Med1* genes. Of course, thyroid hormones regulate metabolic processes and thyroid dysfunction has been reported to be associated with T2DM in several studies. Mice lacking the *Thra* (thyroid hormone receptor-alpha) gene spend more energy in thermogenesis, burn more fat, and are less sensitive to high-fat diet-induced obesity (Pelletier et al. 2008). *MED1* has been shown to act as an essential transcriptional coactivator in adipogenesis, which is an essential function in the development of metabolic disease such as T2D. Adipocyte-specific *Med1* knock-out mice present increased blood glucose and insulin levels, decreased leptin levels and insulin resistance under HFD (Jang et al. 2021). Interestingly the processes involved in the AUC120-180 highly overlap with BGMT180, showcasing a time specific variation.

For the female in fasting glucose levels, *Cbl* is known to mediate insulin-stimulated glucose uptake in adipocyte cells and activation of this pathway is significantly attenuated, during obesity-induced insulin resistance (Liu et al. 2003; Gupte and Mora 2006). *Sik3* is a novel energy regulator that modulates cholesterol and bile acid metabolism (Uebi et al. 2012), and in humans has been found to be downregulated in adipose tissue from obese or insulin-resistant individuals (Säll et al. 2017). *Mpzl3* (myelin protein zero-like 3) encodes a transmembrane protein that has been demonstrated to play an important role in energy balance and knock-out of *Mpzl3* in mice has shown to lead to decreased body weight, increased energy expenditure, reduced blood glucose levels and an enhanced response to insulin (Czyzyk et al. 2013). *Slc37a4* (solute carrier family 37 (glucose-6-phosphate transporter), member 4) is orthologous to human *SLC37A4*, which has been implicated in glycogen storage disorder 1b, which is characterized by an inability to properly metabolize glycogen (Hiraiwa et al. 1999). *Sidt2* (*SID1* transmembrane family, member 2) knock-out mice present with elevated fasting blood glucose and impaired glucose tolerance (Gao et al. 2013).

In AUC0-120 for females, *FTO* harbors the strongest genetic association with polygenic obesity, and *IRX3* mediates the effects of *FTO* on body weight. It has been suggested that macrophage *IRX3* promotes metabolic inflammation to accelerate the development of obesity and type 2 diabetes (Yao et al. 2021). *ARV1* regulates lipid distribution and metabolism in

mammals. *Arv1*^{-/-} mice have been found to be more glucose-tolerant and have increased insulin sensitivity (Gallo-Ebert et al. 2018).

Among the genes prioritized for the female trait AUC0-60, *Sphk1* (sphingosine kinase 1) is a gene, whose role in T2D has been extensively investigated and is summarized in a recent review by Qi et al. (2021). *Acox1* has been suggested as a potential target to improve glucose and lipid homeostasis and tissue response to insulin, in addition to its established anti-inflammatory role (Vamecq et al. 2018), while studies on *ACOX*^{-/-} *ob/ob* mice showed resistance to obesity with improved glucose tolerance and insulin sensitivity (Huang et al. 2012). *GALR2* is crucial to whole-body insulin sensitivity and energy homeostasis, and activation of *GALR2* has been shown to promote glucose metabolism and ameliorate insulin resistance (Fang et al. 2018).

In male mice, there are several genes highlighted in many blood glucose levels and AUC timepoints. On chromosome 11, a cluster of homeobox genes, *Nfe2l1* and *Gip* are prioritized in all blood glucose levels timepoints and AUC0-120, 0-180 and 120-180. *NFE2L1* (also called *Nrf1*) plays a key role in metabolic homeostasis and overexpression of *Nfe2l1* in transgenic mice leads to development of T2D (Hirotsu et al. 2014). *GIP* – also known as glucose-dependent insulinotropic polypeptide – is responsible for insulin secretion in response to nutrients and is a high interest therapeutic target in diabetes and obesity (reviewed in Holst and Rosenkilde 2020). *Phb* on chromosome 11 is prioritized at blood glucose levels timepoints 60 and 120 AUC0-180 and 120-180. *Phb* is of high interest having a role in both immune cells and adipocytes. Transgenic mice overexpressing *Phb* develop obesity in a sex independent manner, but only males develop metabolic dysregulation and diabetes. It is an interesting suggestion that *Phb* leads to development of metabolic disease in male mice through immune dysregulation (Mishra and Nyomba 2017). Finally, *Pdk2* on chromosome 11, is prioritized at BG-T60 and AUC120-180.

On chromosome 9, a cluster of matrix metalloproteinases is prominent in almost all time points (BG-T60, 120 and 180, AUC0-120, 0-180, 60-120 and 30-60). Additionally, *Pgr1*, *Yap1* and *Birc1* and *Birc3* are involved in all blood glucose levels timepoints and AUC0-180, 60-120, 120-180, and 30-60. The progesterone receptor *Pgr* is an interesting finding in male mice. While progesterone has been shown to increase blood glucose levels (Lee et al. 2020) only female and not male *Pgr* knockout mice have improved glucose homeostasis and *Pgr* has been mostly studied in the context of gestational diabetes (Picard et al. 2002). *Yap1* is an important nuclear effector of

the Hippo pathway and has been associated both with the differentiation of insulin-producing β cells, and with glucose utilization through regulation of glucose uptake by Glut1 (Olivieri et al. 2019; Cox et al. 2018). *Birc2* and *Birc3* baculoviral inhibitor genes, which are involved in pancreatic beta cell's stress response and are important in glucose homeostasis (Tan et al. 2013)

Finally, *Mir-1* and *Mir133a*, part of a cluster of miRNAs on chromosome 18, and *Npc1* are prioritized for the trait BG-T120 and AUC0-180, 60-120 and 120-180. *Mir133a* has been extensively studied in diabetic cardiomyopathy where it appears to have a protective effect (Kambis et al. 2019). *Mir1* has been found to mediate IGF-1 signaling (Elia et al. 2009), and to prevent high-fat diet-induced endothelial permeability in apoE knock-out mice (Wang et al. 2013). Additionally, circulating miR-1 and miR-133a levels have been found significantly elevated both in high-fat diet-fed mice and in patients with type 2 diabetes, especially in the presence of myocardial steatosis (de Gonzalo-Calvo et al. 2017). NPC1 is a protein involved in cholesterol efflux from the lysosome. Mice heterozygous or null for *Npc1* are insulin resistant and SNPs within *NPC1* have been associated with obesity and type 2 diabetes (Fletcher et al. 2014).

Most of the QTL mentioned, are associated with impaired glucose tolerance and phenotypes highly relevant to T2D comorbidity, including weight and height, immune response, bone density and colon cancer. We have already published the results of QTL mapping in females with non-alcoholic fatty liver accumulation only (Abu Toamih-Atamni et al. 2016b). Several mechanisms are believed to control obesity and related diseases, including NAFLD and blood glucose levels in both men and women. Also, Human-Mouse Disease Connection (HMDC; <http://www.infomatics.jax.org/humanDisease.shtml>) identifies possible links between our findings in the mouse genome and the corresponding genetic findings in human disease. The search results revealed five human gene homologues (*Wrn/Tex15/Ppp2cb/Gsr/Mboat*) and the *Wrn* and *Mboat* genes were associated with growth/size/body and homeostasis/metabolic phenotypes. Two of the five homologous genes listed above, *Wrn* and *Gsr* are associated with known human diseases, Werner's syndrome, and glutathione reductase disease, respectively. Werner syndrome, caused by the gene encoding the *Wrn* protein, is characterized by a wide range of metabolic/growth complications, including the development of T2D. Glutathione reductase disorders resulting from defects in the gene encoding the *Gsr* protein cause several complications, including cardiovascular and cataract development. These are also known as significant complications of T2D. Overall, a

gene search for the AUC0-180 interval confirms the suitability of using AUC0-180 as a diabetogenic phenotype, as well as the importance of our results to be associated with direct/indirect pathways of T2D.

The CC mouse model has been successfully used in numerous genetic studies, yielding new QTL mapping with high resolution (Vered et al. 2014; Levy et al. 2015; Abu Toamih-Atamni et al. 2016b, 2017, 2019), identification of candidate genes underlying the QTL, next-generation RNA-sequencing for gene expression variations, and estimation of founder effect size by only phenotyping a small number of CC lines (50 CC lines), induced by specific environmental conditions (Abu Toamih-Atamni et al. 2019). Since the wild-derived strains were primarily responsible for the founder effects, it is probable that such a complex disease could not have been understood without these founders. These findings and conclusions were also supported by recent studies using the CC mouse model for various complex traits, including host response to various infectious diseases, such as West Nile virus (Green et al. 2017), influenza A viruses (Elbahesh and Schughartm 2016), and influenza H3N2 (Leist et al. 2016). Based on estimates of founder effects, it was shown that the founder strains with wild ancestry were mostly responsible for the differences between the CC lines after infection. Additionally, analysis of the mapped genomic regions using the mouse genome database (available at <http://www.informatics.jax.org>) showed a number of candidate genes that were strongly linked to host susceptibility.

Finally, we note that in previous studies, investigators typically focused on impaired glucose clearance rather than QTL associated with improved glucose clearance. However, this report is one of the few studies addressing both the phenomenon of impaired glucose clearance and the QTL associated with this trait.

Acknowledgments

This work was supported by the Hendrech and Eiran Gotwert Fund for studying diabetes, Wellcome Trust grants 085906/Z/08/Z, 075491/Z/04 and 090532/Z/09/Z, core funding by Tel-Aviv University (TAU), Israeli Science foundation (ISF) grants 429/09, 961/15 and 1085/18, United States-Israel Binational Science Foundation (BSF) grant 2015077, German Israeli Science Foundation (GIF) grant I-63-410.20-2017. Ilona Binenbaum's PhD thesis was supported by a scholarship from the State Scholarship Foundation in Greece (IKY) (Operational Program "Human Resources Development - Education and Lifelong Learning" Partnership Agreement (PA) 2014–2020).

Author Contribution

Hanifa J. Abu-Toamih-Atamni was involved in the experimental design and execution, data analysis, and drafting the first version of the MS; Iqbal M. Lone was involved in the data analysis and drafting of the MS; Ilona Binenbaum was involved in data analysis and drafting the first version of the MS; Richard Mott was involved in the fundraising, experimental design, bioinformatics analysis, and data mining; Eleftherios Pilalis was involved in bioinformatics analysis; Aristotelis Chatziioannou was involved and supervised all the bioinformatics analysis, data analysis and finalizing the final version of the MS; Fuad A. Iraqi was involved in fundraising for the project, experimental design and execution, data analysis and interpretations, drafting the first version, finalizing the final version of the MS and approving it.

Conflict of Interest

Aristotelis Chatziioannou and Eleftherios Pilalis are co-founders of the e-NIOS Applications PC. Besides that there are no other competing financial interests or associations that might pose a conflict of interest (e.g., pharmaceutical stock ownership, consultancy).

Table and Figure Legends:

Table 1. Summary of significant type 2 Diabetes Specific Locus T2DSL QTL for intraperitoneal glucose tolerance test (IPGTT) traits at age of 20 weeks old mice (following 12 weeks of HFD) for overall population. The levels of genome wide significance thresholds were **95%, *90%.

Table 2. Summary of significant type 2 Diabetes Specific Locus T2DSL QTL for intraperitoneal glucose tolerance test (IPGTT) traits at age of 20 weeks old mice (following 12 weeks of HFD) for males only. The levels of genome wide significance thresholds were **95%, *90%.

Table 3. Summary of significant type 2 Diabetes Specific Locus T2DSL QTL for intraperitoneal glucose tolerance test (IPGTT) traits at 20 weeks old mice (following 12 weeks of HFD) for females only. The levels of genome-wide significance thresholds were **95%, *90%.

Table 4: Summary of significant type 2 Diabetes Specific Locus T2DSL QTL for intraperitoneal glucose tolerance test (IPGTT) traits at age of 20 weeks old mice (following 12 weeks of HFD) with overlapping of the genomic along with their linkage groups on each chromosome indicated by different groups/clusters. The levels of genome-wide significance thresholds were **95%, *90%.

Table 5. Summary of significant type 2 Diabetes Specific Locus T2DSL QTL for intraperitoneal glucose tolerance test (IPGTT) traits at age of 20 weeks old mice (following 12 weeks of HFD) fine mapped by our study. The levels of genome-wide significance thresholds were **95%, *90%.

Figure 1. Total area under the curve (AUC₀₋₁₈₀) of glucose clearance (min*mg/dL) at initial (time 0) and 180 min of intraperitoneal glucose tolerance test (IPGTT) of different CC lines in response to HFD (42 % Fat) dietary challenge. Bar graph (a) shows the IPGTT total AUC of 60 CC lines of the overall CC lines population. Bar graph (b) shows the IPGTT total AUC of females from 45 CC lines. Bar graph (c) shows the total AUC of males from 59 CC lines. A box plot chart summarizes the total AUC values of the different time points, 15, 30, 60, 120, and 180 minutes during the IPGTT, for all CC lines (D). The X-axis represents the line number of different CC lines. The Y-axis represents the total area under the curve of glucose clearance (min*mg/dL) at initial (time 0) and 180 min of intraperitoneal glucose tolerance test (IPGTT).

Figure 1. The AUC at different time points of different CC lines in response to HFD (42 % Fat) dietary challenge. The X-axis represents the line number of different CC lines. The Y-axis represents the total area under the curve of glucose clearance (min*mg/dL) at initial (time 0) and 180 min of intraperitoneal glucose tolerance test (IPGTT).

Figure 2. Genome scan of Quantitative Trait Loci (QTL) associated with total area under the curve of glucose clearance (AUC₀₋₁₈₀ mg/dL*min) trait in the overall population (A), males only (B) and females only (C) in a population of 60 Collaborative Cross (CC) lines after 12 weeks on high-fat (42 % Fat) dietary challenge. The X-axis represents the 19 mouse Chromosomes and the position of mapped QTL on the Chromosome. The Y-axis represents the logP of the association test between locus and AUC₀₋₁₈₀ trait. QTL with logP exceeded the 5.65 threshold, based on permutation genome-wide test, a significant level of $P \leq 0.05$, was identified.

Figure 3. The estimated effect size on the total area under the curve of glucose clearance AUC_{0-180} (mg/dL*min) for the 8 CC founder strains for different Chromosome QTLs in the overall population (**A and B-b**). The X-axis represents eight founder strains of the CC mice. The Y-axis represents the haplotype effect size of the CC founder at the AUC_{0-180} QTL.

Figure 4. The estimated effect size on the total area under the curve of glucose clearance AUC_{0-180} (mg/dL*min) for the 8 CC founder strains for different Chromosome QTL in the male population only (**A and B**). The X-axis represents eight founder strains of the CC mice. The Y-axis represents the haplotype effect size of the CC founder at the AUC_{0-180} QTL.

Figure 5. The estimated effect size on the total area under the curve of glucose clearance AUC_{0-180} (mg/dL*min) for the 8 CC founder strains for different Chromosome QTL in the female population only (**A and B**). The X-axis represents eight founder strains of the CC mice. Y-axis represents the haplotype effect size of the CC founder at the AUC_{0-180} QTL.

Supplementary Table 1. Summary of the used CC lines in our study. The name of each CC line is designated as IL#, and their international CCxxx designation, or if was Extinct, which appears under the column CC lines. Number of males and females in each CC line is provided. Abbreviations: CC, collaborative cross

References.

- Abdelsaid K, Sudhahar V, Harris RA, Das A, Youn SW, Liu Y, McMenamin M, Hou Y, Fulton D, Hamrick MW, Tang Y, Fukai T, Ushio-Fukai M (2022) Exercise improves angiogenic function of circulating exosomes in type 2 diabetes: Role of exosomal SOD3. *FASEB J.*, 36(3):e22177.
- Abu Toamih-Atamni HJ, Mott R, Soller M, Iraqi FA (2016a) High-fat induced development of increased fasting glucose levels and impaired response to intraperitoneal glucose challenge in 123 collaborative cross mouse reference population. *BMC Genet* 17:10
- Abu Toamih-Atamni HJ, Botzman M, Mott R, Gat-Vicks I, Iraqi FA (2016b) Mapping liver fat female-dependent quantitative trait loci in collaborative cross mice. *Mamm. genome.* 27:565-73.
- Abu Toamih-Atamni HJ, Yaron Zinar, Richard Mott, Lior Wolf, and Iraqi FA (2017) Glucose tolerance female-specific QTL mapped in collaborative cross mice. *Mammalian Genome Journal.* 28:20–30. DOI. 10.1007/s00335-016-9667-2.
- Abu-Toamih Atamni HJ, Kontogianni G, Binenbaum I, Mott R, Himmelbauer H, Lehrach H, Chatziioannou A, Iraqi FA (2019) Hepatic gene expression variations in response to diet-induced impaired glucose tolerance using the Collaborative Cross mouse population. *Mammalian Genome* 30(9-10):260-275.
- Allan MF, Eisen EJ, Pomp D (2005) Genomic mapping of direct and correlated responses to long-term selection for rapid growth rate in mice. *Genetics* 170:1863–1877
- American Diabetes Association (ADA) (2021) Classification and diagnosis of diabetes: standards of medical care in diabetes. *Diabetes Care* 44(1):15–33. <https://doi.org/10.2337/dc21-S002>
- Ashburner M, Ball CA, Blake JA, Botstein D, Butler H, Cherry JM, Davis AP, Dolinski K, Dwight SS, Eppig JT, Harris MA, Hill DP, Issel-Tarver L, Kasarskis A, Lewis S, Matese JC, Richardson JE, Ringwald M, Rubin GM, Sherlock G (2000) Gene ontology: a tool for the unification of biology. *Nat Genet* 25(1):25–9
- Bobbala D, Mayhue M, Menendez A, Ilangumaran S, Ramanathan S. Trans-presentation of interleukin-15 by interleukin-15 receptor alpha is dispensable for the pathogenesis of autoimmune type 1 diabetes. *Cell Mol Immunol.* 2017 Jul;14(7):590-596.
- Buse JB, Ginsberg HN, Bakris GL, Clark NG, Costa F, Eckel R (2007) Primary prevention of cardiovascular diseases in people with diabetes mellitus: a scientific statement from the American Heart Association and the American Diabetes Association. *Circulation* 115(1):114–126
- Collin GB, Maddatu TP, Sen S, Naggert JK (2005) Genetic modifiers interact with Cpefat to affect body weight, adiposity, and hyper-glycemia. *Physiol Genom* 22:182–190
- Cox AG, Tsomides A, Yimlamai D, Hwang KL, Miesfeld J, Galli GG, Fowl BH, Fort M, Ma KY, Sullivan MR, Hosios AM, Snay E, Yuan M, Brown KK, Lien EC, Chhangawala S, Steinhauer ML, Asara JM, Houvras Y, Link B, Vander Heiden MG, Camargo FD, Goessling W (2018) Yap regulates glucose utilization and sustains nucleotide synthesis to enable organ growth. *EMBO J.*, 15;37(22):e100294.

- Cox RD, Church CD (2011) Mouse models and the interpretation of human GWAS in type 2 diabetes and obesity. *Dis Model Mech* 4:155–164
- Czyzyk TA, Andrews JL, Coskun T et al. (2013). Genetic ablation of myelin protein zero-like 3 in mice increases energy expenditure, improves glycemic control, and reduces hepatic lipid synthesis. *American Journal of Physiology. Endocrinology and Metabolism*, 305, E282–E292.
- Dagogo-Jack S (2003) Ethnic disparities in type 2 diabetes: pathophysiology and implications for prevention and management. *J Natl Med Assoc* 95:774–789
- De Franco E, Watson RA, Weninger WJ et al. (2019) Specific CNOT1 Mutation Results in a Novel Syndrome of Pancreatic Agenesis and Holoprosencephaly through Impaired Pancreatic and Neurological Development. *Am J Hum Genet*. 104(5):985-989.
- Ding X, Hao Q, Yang M, Chen T, Chen S, Yue J, Leng SX, Dong B (2017) Polymorphism rs189037C > T in the promoter region of the ATM gene may associate with reduced risk of T2DM in older adults in China: a case control study. *BMC Med Genet*. 18(1):84.
- Donath H, Hess U, Kieslich M, Theis M, Ohlenschläger U, Schubert R, Woelke S, Zielen S (2020) Diabetes in Patients With Ataxia Telangiectasia: A National Cohort Study. *Front Pediatr*. 8:317.
- Elbahesh H, Schughart K (2016) Genetically diverse CC-founder mouse strains replicate the human influenza gene expression signature. *Sci Rep* 6:26437
- Elia L, Contu R, Quintavalle M, Varrone F, Chimenti C, Russo MA, Cimino V, De Marinis L, Frustaci A, Catalucci D, Condorelli G (2009) Reciprocal regulation of microRNA-1 and insulin-like growth factor-1 signal transduction cascade in cardiac and skeletal muscle in physiological and pathological conditions. *Circulation*. 120(23):2377-85.
- Fang P, He B, Yu M, Shi M, Zhu Y, Zhang Z, Bo P (2018) Central galanin receptor 2 mediates galanin action to promote systemic glucose metabolism of type 2 diabetic rats. *Biochem Pharmacol*. 156:241-247.
- Fletcher R, Gribben C, Ma X, Burchfield JG, Thomas KC, Krycer JR, James DE, Fazakerley DJ (2014) The role of the Niemann-Pick disease, type C1 protein in adipocyte insulin action. *PLoS One*. 9(4):e95598.
- Flisiak-Jackiewicz M, Bobrus-Chociej A, Wasilewska AN, Lebensztejn DM (2021) From nonalcoholic fatty liver disease (NAFLD) to metabolic dysfunction-associated fatty liver disease (MAFLD)— new terminology in pediatric patients as a step in good scientific direction? *J Clin Med* 10:924. https://doi.org/10.3390/jcm10_050924
- Gallo-Ebert C, Francisco J, Liu HY, Draper R, Modi K, Hayward MD, Jones BK, Buiakova O, McDonough V, Nickels JT Jr (2018) Mice lacking **ARV1** have reduced signs of metabolic syndrome and non-alcoholic fatty liver disease. *J Biol Chem*. 293(16):5956-5974.
- Gao J, Gu X, Mahuran DJ, Wang Z, Zhang H (2013) Impaired glucose tolerance in a mouse model of *sirt2* deficiency. *PLoS One*. 8(6):e66139
- García-Tornadú I, Ornstein AM, Chamson-Reig A, Wheeler MB, Hill DJ, Arany E, Rubinstein M, Becu-Villalobos D (2010) Disruption of the dopamine d2 receptor impairs insulin secretion and causes glucose intolerance. *Endocrinology*. 151(4):1441-50.

Garg G, Tyler JR, Yang JH, Cutler AJ, Downes K, Pekalski M, Bell GL, Nutland S, Peakman M, Todd JA, Wicker LS, Tree TI (2012) Type 1 diabetes-associated IL2RA variation lowers IL-2 signaling and contributes to diminished CD4⁺CD25⁺ regulatory T cell function. *J Immunol.* 188(9):4644-53.

de Gonzalo-Calvo D, van der Meer RW, Rijzewijk LJ, Smit JW, Revuelta-Lopez E, Nasarre L, Escola-Gil JC, Lamb HJ, Llorente-Cortes V (2017) Serum microRNA-1 and microRNA-133a levels reflect myocardial steatosis in uncomplicated type 2 diabetes. *Sci Rep.* 7(1):47.

Ghnaim A, Lone IM, Ben-Nun N, Iraqi FA (2023) Unraveling the Host Genetic Background Effect on Internal Organ Weight Influenced by Obesity and Diabetes Using Collaborative Cross Mice. *Int. J. Mol. Sci.* 24, 8201.

Gillespie M, Jassal B, Stephan R, Milacic M, Rothfels K, Senff-Ribeiro A, Griss J, Sevilla C, Matthews L, Gong C, Deng C, Varusai T, Ragueneau E, Haider Y, May B, Shamovsky V, Weiser J, Brunson T, Sanati N, Beckman L, Shao X, Fabregat A, Sidiropoulos K, Murillo J, Viteri G, Cook J, Shorser S, Bader G, Demir E, Sander C, Haw R, Wu G, Stein L, Hermjakob H, D'Eustachio P (2022) The reactome pathway knowledge base 2022. *Nucleic Acids Res.* 50(D1):D687-D692.

Green R, Wilkins C, Thomas S, Sekine A, Hendrick DM, Voss K et al. (2017) Oas1b-dependent immune transcriptional profiles of West Nile virus infection in the Collaborative Cross. *G3 (Bethesda)* 7(6):1665–1682

Gupte A, Mora S (2006) Activation of the Cbl insulin signaling pathway in cardiac muscle; dysregulation in obesity and diabetes. *Biochem Biophys Res Commun.* 342(3):751-7.

Hecker PA, Mapanga RF, Kimar CP, Ribeiro RF Jr, Brown BH, O'Connell KA, Cox JW, Shekar KC, Asemu G, Essop MF, Stanley WC (2012) Effects of glucose-6-phosphate dehydrogenase deficiency on the metabolic and cardiac responses to obesogenic or high-fructose diets. *Am J Physiol Endocrinol Metab.* 303(8):E959-72.

Hiraiwa H, Pan CJ, Lin B, Moses SW, Chou JY (1999) Inactivation of the glucose 6-phosphate transporter causes glycogen storage disease type 1b. *J. Biol. Chem.* 274:5532–5536.

Hirayama I, Yi Z, Izumi S, Arai I, Suzuki W, Nagamachi Y, Kuwano H, Takeuchi T, Izumi T (1999) Genetic analysis of obese diabetes in the TSOD mouse. *Diabetes* 48:1183–1191

Hirotsu Y, Higashi C, Fukutomi T, Katsuoka F, Tsujita T, Yagishita Y, Matsuyama Y, Motohashi H, Uruno A, Yamamoto M (2014) Transcription factor NF-E2-related factor 1 impairs glucose metabolism in mice. *Genes Cells.* 19(8):650-65.

Holst JJ, Rosenkilde MM (2020) GIP as a Therapeutic Target in Diabetes and Obesity: Insight From Incretin Co-agonists. *J Clin Endocrinol Metab.* 105(8):e2710–6.

Huang J, Jia Y, Fu T, Viswakarma N, Bai L, Rao MS, Zhu Y, Borensztajn J, Reddy JK (2012) Sustained activation of PPAR α by endogenous ligands increases hepatic fatty acid oxidation and prevents obesity in ob/ob mice. *FASEB J.* 26(2):628-38.

Iraqi F, Churchill G, Mott R (2008) The Collaborative Cross, developing a resource for mammalian systems genetics: a status report of the welcome trust COHORT. *Mamm Genome* 19:379–381

- Iraqi FA, Mahajne M, Salaymah A, Sandovsky H, Tayem H et al (2012) The genome architecture of the collaborative cross mouse genetic reference population collaborative cross consortium. *Genetics* 190:389–402
- Jang Y, Park YK, Lee JE, Wan D, Tran N, Gavrilova O, Ge K (2021) MED1 is a lipogenesis coactivator required for postnatal adipose expansion. *Genes Dev.* 35(9-10):713-728.
- Jetten AM, Kang HS, Takeda Y (2013) Retinoic acid-related orphan receptors α and γ : key regulators of lipid/glucose metabolism, inflammation, and insulin sensitivity. *Front Endocrinol (Lausanne)*. 4:1. S
- Kambis TN, Shahshahan HR, Kar S, Yadav SK, Mishra PK (2019) Transgenic expression of miR-133a in the diabetic akita heart prevents cardiac remodeling and cardiomyopathy. *Frontiers in cardiovascular medicine*. 6:45.
- Kaul N, Ali S (2016) Genes, genetics, and environment in type 2 diabetes: Impl. *DNA Cell Biol* 35(1):1–12
- Khatib MN, Gaidhane S, Gaidhane AM, Simkhada P, Zahiruddin QS (2015) Ghrelin O Acyl Transferase (GOAT) as a Novel Metabolic Regulatory Enzyme. *J Clin Diagn Res.* 9(2):LE01-5.
- Koutsandreas T, Binenbaum I, Pilalis E, Valavanis I, Papadodima O, Chatziioannou A (2016) Analyzing and visualizing genomic complexity for the derivation of the emergent molecular networks. *Int J Monit Surveill Technol Res* 4(2):30–49
- Lee SR, Choi WY, Heo JH, Huh J, Kim G, Lee KP, Kwun HJ, Shin HJ, Baek IJ, Hong EJ (2020) Progesterone increases blood glucose via hepatic progesterone receptor membrane component 1 under limited or impaired action of insulin. *Sci Rep.* 10(1):16316.
- Lehman DM, Hamlington J, Hunt KJ, Leach RJ, Arya R, Abboud H, Duggirala R, Blangero J, Göring HH, Stern MP(2006) A novel missense mutation in ADRB3 increases risk for type 2 diabetes in a Mexican American family. *Diabetes Metab Res Rev.* 22(4):331-6
- Leiter EH (2009) Selecting the “Right” mouse model for metabolic syndrome and type 2 diabetes. T2 diabetes. *Methods Mol Biol* 560:1–17
- Leiter EH, Reifsnyder PC, Flurkey K, Partke HJ, Junger E, Herberg L (1998) NIDDM genes in mice: deleterious synergism by both parental genomes contributes to diabetogenic thresholds. *Diabetes* 47:1287–1295
- Levy R, Mott R, Iraqi FA, Gabetp Y (2015) Collaborative cross mice in a genetic association study reveal new candidate genes for bone microarchitecture. *BMC Genom* 16(1013):1–14
- Lian J, Nelson R, Lehner R (2018) Carboxylesterases in lipid metabolism: from mouse to human. *Protein Cell.* 9(2):178-195.
- Ling W, Huang Y, Huang YM et al (2020) Global trend of diabetes mortality attributed to vascular complications, 2000–2016. *Cardiovasc Diabetol* 19:182
- Liu J, DeYoung SM, Hwang JB, O'Leary EE, Saltiel AR (2003) The roles of Cbl-b and c-Cbl in insulin-stimulated glucose transport. *J Biol Chem.* 278(38):36754-62.

Leist SR, Pilzner C, van den Brand JM, Dengler L, Geffers R, Kuiken T et al (2016) Influenza H3N2 infection of the collaborative cross founder strains reveals highly divergent host responses and identifies a unique phenotype in CAST/EiJ mice. *BMC Genomics* 17:143

Lone IM, Iraqi FA (2022) Genetics of Murine Type 2 Diabetes and Comorbidities. *Mamm. Genome* 2022, 33, 421–436.

Lone IM, Ben Nun N, Ghnaim A, Schaefer AS, Hourri-Haddad Y, Iraqi FA (2023b) High-Fat Diet and Oral Infection Induced Type 2 Diabetes and Obesity Development under Different Genetic Backgrounds. *Anim. Model. Exp. Med.* 6, 131–145.

Lone IM, Zohud O, Nashef A, Kirschneck C, Proff P, Watted N, Iraqi FA (2023c) Dissecting the Complexity of Skeletal-Malocclusion-Associated Phenotypes: Mouse for the Rescue. *Int. J. Mol. Sci.* 24, 2570.

Lone IM, Midlej K, Ben Nun N, Iraqi FA (2023a) Intestinal Cancer Development in Response to Oral Infection with High-Fat Diet-Induced Type 2 Diabetes (T2D) in Collaborative Cross Mice under Different Host Genetic Background Effects. *Mamm. Genome* 34, 56–75.

Mathers CD, Loncar D (2006) Projections of global mortality and burden of disease from 2002 to 2030. *PLoS Med* 3(11):442

Miles PD, Treuner K, Latronica M, Olefsky JM, Barlow C (2007) Impaired insulin secretion in a mouse model of ataxia telangiectasia. *Am J Physiol Endocrinol Metab.* 293(1):E70-4.

Mishra S, Nyomba BG (2017) Prohibitin - At the crossroads of obesity-linked diabetes and cancer. *Exp Biol Med (Maywood).* 242(11):1170-1177.

Mohlke KL, Boehnke M (2015) Recent advances in understanding the genetic architecture of type 2 diabetes. *Hum Mol Genet* 24:R85

Montgomery MK, Hallahan NL, Brown SH et al (2013) Mouse strain-independent variation in obesity and glucose homeostasis in response to high-fat-feeding. *Diabetologia* 56:1129–1139

Pelletier P, Gauthier K, Sideleva O, Samarut J, Silva JE (2008) Mice lacking the thyroid hormone receptor-alpha gene spend more energy in thermogenesis, burn more fat, and are less sensitive to high-fat diet-induced obesity. *Endocrinology.* 149(12):6471-86.

Picard F, Wanatabe M, Schoonjans K, Lydon J, O'Malley BW, Auwerx J (2002) Progesterone receptor knockout mice have an improved glucose homeostasis secondary to beta-cell proliferation. *Proc Natl Acad Sci U S A.* 99(24):15644-8.

Qi Y, Wang W, Song Z, Aji G, Liu XT, Xia P (2021) Role of Sphingosine Kinase in Type 2 Diabetes Mellitus. *Front Endocrinol (Lausanne).* 11:627076.

Quinn LS, Anderson BG (2011) Interleukin-15, IL-15 Receptor-Alpha, and Obesity: Concordance of Laboratory Animal and Human Genetic Studies. *J Obes.* 2011:456347.

Ramachandrappa S, Farooqi IS (2011) Genetic approaches to understanding human obesity. *J Clin Investig* 121(6):2080–2086

Reaven GM (1988) Banting lecture 1988 Role of insulin resistance in human disease. *Diabetes* 37:1595–1607

Rosado-Olivieri EA, Anderson K, Kenty JH, Melton DA (2019) YAP inhibition enhances the differentiation of functional stem cell-derived insulin-producing β cells. *Nat Commun.* 10(1):1464.

- Saeedi P, Petersohn I, Salpea P, Malanda B, Karuranga S, Unwin N, Colagiuri S, Guariguata L, Motala AA, Ogurtsova K, Shaw JE, Bright D, Williams R (2019) Global and regional diabetes prevalence estimates for 2019 and projections for 2030 and 2045: Results from the International Diabetes Federation Diabetes Atlas, 9th edition. *Diabetes Res Clin Pract.* <https://doi.org/10.1016/j.diabres.2019.107843>
- Säll J, Pettersson AM, Björk C, Henriksson E, Wasserstrom S, Linder W, Zhou Y, Hansson O, Andersson DP, Ekelund M, Degerman E, Stenkula KG, Laurencikiene J, Göransson O (2017) Salt-inducible kinase 2 and -3 are downregulated in adipose tissue from obese or insulin-resistant individuals: implications for insulin signalling and glucose uptake in human adipocytes. *Diabetologia.* 60(2):314-323.
- Samsom M, Trivedi T, Orekoya O, Vyas S (2016) Understanding the importance of gene and environment in the etiology and prevention of type 2 diabetes mellitus in high-risk populations. *Oral Health Case Rep.* 2(1):112
- Sandholt CH, Hansen T, Pedersen O (2012) Beyond the fourth wave of genome-wide obesity association studies. *Nutr Diabetes* 2(7):e37. <https://doi.org/10.1038/nutd.2012.9>. PMID:23168490; PMCID:PMC3408643
- Shike T, Hirose S, Kobayashi M, Funabiki K, Shirai T, Tomino Y (2001) Susceptibility and negative epistatic loci contributing to type 2 diabetes and related phenotypes in a KK/Ta mouse model. *Diabetes* 50:1943–1948
- Smith CL, Eppig JT (2012) The mammalian phenotype ontology as a unifying standard for experimental and high-throughput phenotyping data. *Mamm Genome* 23(9–10):653–68
- Smith Richards BK, Belton BN, Poole AC, Mancuso JJ, Churchill GA, Li R, Volaufova J, Zuberi A, York B (2002) QTL analysis of self-selected macronutrient diet intake: fat, carbohydrate, and total kilocalories. *Physiol Genom* 11:205–217
- Stoehr JP, Nadler ST, Schueler KL, Rabaglia ME, Yandell BS, Metz SA, Attie AD (2000) Genetic obesity unmasks nonlinear interactions between murine type 2 diabetes susceptibility loci. *Diabetes* 49:1946–1954
- Sudhakar V, Urao N, Oshikawa J, McKinney RD, Llanos RM, Mercer JF, Ushio-Fukai M, Fukui T (2013) Copper transporter ATP7A protects against endothelial dysfunction in type 1 diabetic mice by regulating extracellular superoxide dismutase. *Diabetes.* 62(11):3839-50.
- Tan BM, Zammit NW, Yam AO, Slattery R, Walters SN, Malle E, Grey ST (2013) Baculoviral inhibitors of apoptosis repeat containing (BIRC) proteins fine-tune TNF-induced nuclear factor κ B and c-Jun N-terminal kinase signalling in mouse pancreatic beta cells. *Diabetologia.* 56(3):520-32.
- Toye AA, Lippiat JD, Proks P, Shimomura K, Bentley L, Hugill A, Mijat V, Goldsworthy M, Moir L, Haynes A, Quarterman J, Freeman HC, Ashcroft FM, Cox RD (2005) A genetic and physiological study of impaired glucose homeostasis control in C57BL/6J mice. *Diabetologia* 48:675–686
- Uebi T, Itoh Y, Hatano O, Kumagai A, Sanosaka M, Sasaki T, Sasagawa S, Doi J, Tatsumi K, Mitamura K, Morii E, Aozasa K, Kawamura T, Okumura M, Nakae J, Takikawa H, Fukusato T, Koura M, Nish M, Hamsten A, Silveira A, Bertorello AM, Kitagawa K, Nagaoka Y, Kawahara H,

- Tomonaga T, Naka T, Ikegawa S, Tsumaki N, Matsuda J, Takemori H (2012) Involvement of SIK3 in glucose and lipid homeostasis in mice. *PLoS One*. 7(5):e37803.
- Valiquette, Guy (2011). Bromocriptine for Diabetes Mellitus Type II. *Cardiology in Review*, 19(6), 272–275.
- Vamecq J, Andreoletti P, El Kebbjaj R, Saih FE, Latruffe N, El Kebbjaj MHS, Lizard G, Nasser B, Cherkaoui-Malki M (2018) Peroxisomal Acyl-CoA Oxidase Type 1: Anti-Inflammatory and Anti-Aging Properties with a Special Emphasis on Studies with LPS and Argan Oil as a Model Transposable to Aging. *Oxid Med Cell Longev*. 2018:6986984.
- Vered K, Durrant C, Mott R, Iraqi FA (2014) Susceptibility to *Klebsiella pneumoniae* infection in collaborative cross mice is a complex trait controlled by at least three loci acting at different time points. *BMC Genom* 15:865
- Walston J, Silver K, Bogardus C, Knowler WC, Celi FS, Austin S, Manning B, Strosberg AD, Stern MP, Raben N, et al (1995) Time of onset of non-insulin-dependent diabetes mellitus and genetic variation in the beta 3-adrenergic-receptor gene. *N Engl J Med*. 333(6):343-7.
- Wang H, Zhu HQ, Wang F, Zhou Q, Gui SY, Wang Y (2013) MicroRNA-1 prevents high-fat diet-induced endothelial permeability in apoE knock-out mice. *Mol Cell Biochem*. 378(1-2):153-9.
- Wild S, Roglic G, Green A, Sicree R, King H (2004) Global prevalence of diabetes: estimates for the year 2000 and projections for 2030. *Diabetes Care* 27(5):1047–1053
- Wilson CH, Kumar S (2018) Caspases in metabolic disease and their therapeutic potential. *Cell Death Differ*. 25(6):1010-1024.
- Yang L, Li H, Yu T, Zhao H, Cherian MG, Cai L, Liu Y (2008) Polymorphisms in metallothionein-1 and -2 genes associated with the risk of type 2 diabetes mellitus and its complications. *Am J Physiol Endocrinol Metab*. 294(5):E987-92.
- Yang H, Ding Y, Hutchins LN, Szatkiewicz J, Bell TA et al (2009) A customized and versatile high-density genotyping array for the mouse. *Nat Methods* 6:663–666
- Yao J, Wu, D., Zhang C, et al (2021) Macrophage IRX3 promotes diet-induced obesity and metabolic inflammation. *Nat Immunol* 22, 1268–1279.
- Yehi, R, Lone IM, Yehia I, Iraqi FA (2023) Studying the Pharmagenomic Effect of *Portulaca Oleracea* Extract on Anti-Diabetic Therapy Using the Collaborative Cross Mice. *Phytomed*. Plus 3, 100394.
- Yi W, Clark PM, Mason DE, Keenan MC, Hill C, Goddard WA 3rd, Peters EC, Driggers EM, Hsieh-Wilson LC (2012) Phosphofructokinase 1 glycosylation regulates cell growth and metabolism. *Science*. 337(6097):975-80.
- Zhou J, Wu T, Li C, Hu Z, Han L, Li X, Liu J, Zhao W, Kang J, Chen X (2023) Alifuzosin ameliorates diabetes by boosting PGK1 activity in diabetic mice. *Life Sci*. 317:121491.
- Harries LW, Hattersley AT, Doney AS, Colhoun H, Morris AD, Sutherland C, Hardie DG, Peltonen L, McCarthy MI, Holman RR (2011) Common variants near ATM are associated with glycemic response to metformin in type 2 diabetes. *Nature genetics*. 43(2):117-20.

Diaferia RG, Jimenez-Caliani JA, Ranjitkar P, Yang W, Hardiman G, Rhodes JC, Crisa L, Vincenzo Cirulli V (2013) β 1 integrin is a crucial regulator of pancreatic β -cell expansion. *Development*. 140(16):3360-72.

Guigas B, de Leeuw van Weenen EJ, van Leeuwen N, Simonis-Bik MA, van Haefen WT, Nijpels G, Duistermaat JJ, Beekman M, Deelen J, Havekes ML, Penninx WB, et al. (2014) Sex-specific effects of naturally occurring variants in the dopamine receptor D2 locus on insulin secretion and Type 2 diabetes susceptibility. *Diabetic Medicine*. 31(8): 1001-1008.

He HJ, Kole S, Kwon YK, Crow MT, Bernier M. Interaction of filamin A with the insulin receptor alters insulin-dependent activation of the mitogen-activated protein kinase pathway. *J Biol Chem*. 2003 Jul 18;278(29):27096-104.

Table 1. Overall population

Trait	Chr	QTL	Peak (Mb)	50% CI (Mb) Size (Mb) (Genes)	90% CI (Mb) Size (Mb)(Genes)	95% CI (Mb) Size (Mb)(Genes)
Fasting Glucose (BG-T0)	ChrX	T2DSL1**	100.09	99.79-100.45 0.66 (9)	99.04-107.10 8.05 (233)	98.61-108.30 9.69 (252)
	Chr2	T2DSL2**	15.64	15.18-16.06 0.88 (7)	12.91-17.90 4.99 (63)	12.17-19.25 7.08 (100)
BG - T180	Chr8	T2DSL3**	112.96	112.55-113.59 1.04 (8)	110.37-115.19 4.82 (81)	109.29-115.92 6.64 (119)
	Chr14	T2DSL4**	79.26	79.05-79.53 0.48 (16)	78.30-80.68 2.38 (40)	77.95-81.22 3.27 (46)
		T2DSL5**	86.64	86.35-87.13 0.78 (2)	84.62-89.08 4.46 (16)	83.94-89.71 5.76 (21)
	Chr11	T2DSL6*	97.16	96.84-97.45 0.61 (31)	95.60-98.62 3.01 (146)	94.96-99.60 4.46 (221)
	Chr17	T2DSL7*	90.78	90.41-90.97 0.56 (8)	89.57-91.96 2.39 (21)	89.05-92.58 3.53 (27)
AUC 0-120	Chr8	T2DSL8**	96.04	95.89-96.25 0.36 (2)	95.46-96.93 1.47 (22)	95.31-97.32 2.02 (30)
		T2DSL9**	130.18	129.57-130.65 1.08 (0)	126.50-132.28 5.79 (35)	125.71-132.88 7.17 (45)

AUC 120-180	Chr8	T2DSL10*	112.96	112.59-113.36 0.77 (3)	111.14-114.29 3.15 (48)	110.36-114.77 4.40 (79)
	Chr11	T2DSL11*	97.08	96.84-97.33 0.48 (29)	95.99-98.25 2.26 (110)	95.44-99.06 3.62 (176)

Table 2. Males only

Trait	Chr	QTL	Peak (Mb)	50% CI (Mb) Size (Mb) (Genes)	90% CI (Mb) Size (Mb) (Genes)	95% CI (Mb) Size (Mb) (Genes)
Fasting Glucose (BG-T0)	Chr2	T2DSL12**	15.53	15.10-15.91 0.81 (6)	13.07-17.80 4.73 (59)	11.54-19.02 7.48 (107)
BG-T60	Chr9	T2DSL13**	9.09	8.79-9.28 0.49 (4)	7.65-10.50 2.85 (33)	7.14-11.46 4.33 (48)
	Chr11	T2DSL14*	95.92	95.74-96.05 0.31 (17)	95.23-96.53 1.30 (59)	94.98-96.84 1.87 (78)
BG-T120	Chr11	T2DSL15*	96.48	96.30-96.67 0.37 (13)	95.68-97.52 1.84 (89)	95.21-98.00 2.79 (127)
	Chr9	T2DSL16**	9.09	8.74-9.40 0.66 (5)	7.01-11.06 4.05 (48)	5.94-12.30 6.37 (57)
	Chr18	T2DSL17**	12.26	11.54-12.71 1.18 (22)	8.19-14.28 6.09 (94)	6.67-15.70 9.03 (134)
BG-T180	Chr14	T2DSL18**	86.67	86.16-87.26 1.10 (5)	84.27-89.73 5.46 (21)	83.75-91.22 7.47 (28)
		T2DSL19*	79.64	79.38-80.05 0.67 (17)	78.40-81.74 3.34 (41)	77.98-82.70 4.71 (52)
	Chr8	T2DSL20*	112.83	112.53-113.06 0.53 (3)	111.96-113.59 1.64 (18)	111.66-113.87 2.21 (31)
	Chr9	T2DSL21*	10.77	10.20-11.18 0.97 (6)	7.16-13.55 6.39 (58)	6.38-14.23 7.85 (69)
		T2DSL22*	6.01	5.49-6.61 1.11 (7)	2.98-9.33 6.35 (84)	2.23-10.34 8.11 (88)
	Chr11	T2DSL23*	97.84	97.44-98.09 0.64 (36)	96.22-99.16 2.93 (144)	95.72-100.04 4.32 (256)
AUC0-180	Chr9	T2DSL24**	9.09	8.83-9.31 0.48 (5)	7.48-10.52 3.04 (36)	6.77-11.48 4.71 (49)
		T2DSL25**	51.05	50.81-51.18 0.37 (10)	50.16-51.80 1.64 (41)	49.71-52.16 2.44 (51)
	Chr11	T2DSL26**	96.43	96.22-96.60 0.38 (20)	95.62-97.12 1.50 (78)	95.23-97.47 2.24 (98)

	Chr5	T2DSL27*	140.22	139.99-140.42 0.43 (9)	139.00-141.02 2.02 (48)	138.40-141.26 2.86 (62)
	Chr18	T2DSL28*	12.26	12.01-12.50 0.50 (12)	10.80-13.30 2.50 (41)	9.96-13.71 3.75 (66)
AUC0-120	Chr11	T2DSL29**	96.48	96.30-96.64 0.34 (13)	95.95-97.15 1.21 (64)	95.68-97.52 1.83 (89)
	Chr1	T2DSL30*	61.80	61.68-61.91 0.23 (0)	61.21-62.37 1.17 (17)	60.62-62.82 2.20 (60)
	Chr8	T2DSL31*	96.04	95.91-96.27 0.36 (2)	95.41-97.30 1.89 (26)	94.89-98.01 3.12 (43)
AUC30-60	Chr9	T2DSL32**	9.09	8.94-9.25 0.31 (4)	7.84-10.25 2.40 (21)	7.41-11.47 4.06 (42)
AUC60-120	Chr9	T2DSL33**	9.09	8.87-9.30 0.43 (5)	7.56-10.63 3.07 (35)	6.99-11.85 4.86 (49)
	Chr5	T2DSL34*	140.22	140.01-140.38 0.38 (8)	139.14-141.00 1.85 (47)	138.51-141.18 2.66 (59)
	Chr18	T2DSL35*	12.26	11.94-12.53 0.59 (12)	10.45-13.38 2.92 (55)	9.08-13.90 4.82 (86)
AUC120-180	Chr9	T2DSL36**	11.25	10.89-11.54 0.65 (4)	8.92-13.53 4.62 (23)	7.83-14.28 6.45 (48)
		T2DSL37**	51.12	50.64-51.42 0.78 (22)	48.92-52.72 3.79 (67)	48.11-54.09 5.98 (104)
	Chr11	T2DSL38**	96.48	96.24-96.68 0.45 (21)	95.39-97.33 1.94 (90)	94.91-97.84 2.94 (136)
	Chr14	T2DSL39**	79.66	79.36-80.00 0.64 (18)	78.35-81.25 2.91 (39)	77.98-82.24 4.26 (50)
	Chr18	T2DSL40*	12.26	12.08-12.45 0.37 (10)	11.34-12.99 1.65 (3 0)	10.84-13.31 2.47 (49)
	Chr19	T2DSL41*	50.20	49.93-50.39 0.46 (2)	49.34-50.87 1.53 (5)	49.05-51.16 2.11 (5)
	ChrX	T2DSL42*	77.18	76.54-77.63 1.09 (14)	74.83-82.62 7.78 (138)	74.20-84.33 10.13 (194)

Table 3. Females only

Trait	Chr	QTL	Peak (Mb)	<u>50% CI(Mb)</u> Size (Mb) (Genes)	<u>90% CI(Mb)</u> Size (Mb) (Genes)	<u>95% CI(Mb)</u> Size (Mb) (Genes)
Fasting Glucose (BG-T0)	Chr9	T2DSL43*	44.39	44.03-44.57 0.55 (38)	42.70-45.76 3.06 (93)	42.13-46.37 4.24 (126)
AUC0-120	Chr8	T2DSL44**	129.73	128.19-130.31 2.13 (17)	122.86-132.85 9.99 (181)	120.64-133.55 12.91 (242)
		T2DSL45*	94.47	94.17-95.25 1.08 (39)	92.09-98.32 6.23 (105)	88.66-99.48 10.82 (147)
AUC0-60	Chr11	T2DSL46**	116.64	116.46-116.81 0.35 (21)	115.88-117.30 1.42 (70)	115.72-117.51 1.79 (83)

****95%, *90% levels of genome-wide significance thresholds**

Table 4.

Trait	Chr	Fine Mapped QTL	Peak (Mb)	95% CI (Mb) Size (Mb)(Genes)	Previously identified QTL	Genomic interval (Mb)
Mapped QTL in the overall population						
Fasting Glucose (BG-T0)	ChrX	T2DSL1**	100.09	98.61-108.30 9.69 (252)	<i>Mnic3</i>	98.05–160.60
BG - T180	Chr8	T2DSL3**	112.96	109.29-115.92 6.64 (119)	<i>Tg1</i>	86.69–125.14
	Chr11	T2DSL6*	97.16	94.96-99.60 4.46 (221)	<i>Mglcq1</i>	82.37–122.05
AUC 0-120	Chr8	T2DSL8**	96.04	95.31-97.32 2.02 (30)	<i>Tg1</i>	86.69–125.14
AUC 120-180	Chr8	T2DSL10*	112.96	110.36-114.77 4.40 (79)	<i>Tg1</i>	86.69–125.14
	Chr11	T2DSL11*	97.08	95.44-99.06 3.62 (176)	<i>Nidd4</i>	94.18–121.60
Mapped QTL in males only						
BG-T60	Chr11	T2DSL14*	95.92	94.98-96.84 1.87 (78)	<i>Nidd4</i>	94.18–121.60
BG-T120	Chr11	T2DSL15*	96.48	95.21-98.00 2.79 (127)	<i>Nidd4</i>	94.18–121.60
	Chr18	T2DSL17**	12.26	6.67-15.70 9.03 (134)	<i>Nidd2</i>	12.11–45.03

BG-T180	Chr8	T2DSL20*	112.83	111.66-113.87 2.21 (31)	<i>Tg1</i>	86.69–125.14
	Chr11	T2DSL23*	97.84	95.72-100.04 4.32 (256)	<i>Mglcq1</i>	82.37–122.05
AUC0-180	Chr9	T2DSL25**	51.05	49.71-52.16 2.44 (51)	<i>Gluchos</i>	19.61–59.29
	Chr11	T2DSL26**	96.43	95.23-97.47 2.24 (98)	<i>Nidd4</i>	94.18–121.60
	Chr5	T2DSL27*	140.22	138.40-141.26 2.86 (62)	<i>Find2</i>	105.28–144.96
	Chr18	T2DSL28*	12.26	9.96-13.71 3.75 (66)	<i>Nidd2</i>	12.11–45.03
AUC0-120	Chr11	T2DSL29**	96.48	95.68-97.52	<i>Mglcq1</i>	82.37–122.05
				1.83 (89)		
	Chr8	T2DSL31*	96.04	94.89-98.01 3.12 (43)	<i>Tg1</i>	86.69–125.14
AUC60-120	Chr5	T2DSL34*	140.22	138.51-141.18 2.66 (59)	<i>Find2</i>	105.28–144.96
	Chr18	T2DSL35*	12.26	9.08-13.90 4.82 (86)	<i>Nidd2</i>	12.11–45.03
AUC120-180	Chr9	T2DSL37**	51.12	48.11-54.09 5.98 (104)	<i>Gluchos</i>	19.61–59.29
	Chr11	T2DSL38**	96.48	94.91-97.84 2.94 (136)	<i>Nidd4</i>	94.18–121.60
	Chr18	T2DSL40*	12.26	10.84-13.31 2.47 (49)	<i>Nidd2</i>	12.11–45.03
	Chr19	T2DSL41*	50.20	49.05-51.16 2.11 (5)	<i>Tannid1</i>	26.02–59.05

Mapped QTL in females only						
Fasting Glucose (BG-T0)	Chr9	T2DSL43*	44.39	42.13-46.37 4.24 (126)	<i>Glucos</i>	19.61–59.29
AUC0-120	Chr8	T2DSL44**	129.73	120.64-133.55 12.91 (242)	<i>Tg1</i>	86.69–125.14
		T2DSL45*	94.47	88.66-99.48 10.82 (147)	<i>Tg1</i>	86.69–125.14
AUC0-60	Chr11	T2DSL46**	116.64	115.72-117.51 1.79 (83)	<i>Dbm2</i>	101.36–117.94

Table 5.

Tested traits and status	Shared loci of multiple traits	Chr.	QTL	Peak (Mb)	50% CI (Mb) Size (Mb) (Genes)	90% CI (Mb) Size (Mb) (Genes)	95% CI (Mb) Size (Mb) (Genes)
Fasting Glucose (BG-T0)-overall	1	Chr2	T2DSL2**	15.64	15.18-16.06 0.88 (7)	12.91-17.90 4.99 (63)	12.17-19.25 7.08 (100)
Fasting Glucose (BG-T0)-males	1	Chr2	T2DSL12* *	15.53	15.10-15.91 0.81 (6)	13.07-17.80 4.73 (59)	11.54-19.02 7.48 (107)
AUC0-180-overall	2	Chr5	T2DSL27*	140.22	139.99-140.42 0.43 (9)	139.00-141.02 2.02 (48)	138.40-141.26 2.86 (62)
AUC60-120-males	2	Chr5	T2DSL34*	140.22	140.01-140.38 0.38 (8)	139.14-141.00 1.85 (47)	138.51-141.18 2.66 (59)
BG - T180-overall	3	Chr8	T2DSL3**	112.96	112.55-113.59 1.04 (8)	110.37-115.19 4.82 (81)	109.29-115.92 6.64 (119)
AUC 120-180-overall	3	Chr8	T2DSL10*	112.96	112.59-113.36 0.77 (3)	111.14-114.29 3.15 (48)	110.36-114.77 4.40 (79)
BG-T180-male	3	Chr8	T2DSL20*	112.83	112.53-113.06 0.53 (3)	111.96-113.59 1.64 (18)	111.66-113.87 2.21 (31)
AUC0-120-male	4	Chr8	T2DSL31*	96.04	95.91-96.27 0.36 (2)	95.41-97.30 1.89 (26)	94.89-98.01 3.12 (43)
AUC 0-120-overall	4	Chr8	T2DSL8**	96.04	95.89-96.25 0.36 (2)	95.46-96.93 1.47 (22)	95.31-97.32 2.02 (30)
AUC0-120-femal	4	Chr8	T2DSL45*	94.47	94.17-95.25 1.08 (39)	92.09-98.32 6.23 (105)	88.66-99.48 10.82 (147)
AUC0-120-female	5	Chr8	T2DSL44* *	129.73	128.19-130.31	122.86-132.85	120.64-133.55

					2.13 (17)	9.99 (181)	12.91 (242)
AUC0-120- overall	5	Chr8	T2DSL9**	130.18	129.57-130.65 1.08 (0)	126.50-132.28 5.79 (35)	125.71-132.88 7.17 (45)
BG-T60-male	6	Chr9	T2DSL13* *	9.09	8.79-9.28 0.49 (4)	7.65-10.50 2.85 (33)	7.14-11.46 4.33 (48)
BG-T120-male	6	Chr9	T2DSL16* *	9.09	8.74-9.40 0.66 (5)	7.01-11.06 4.05 (48)	5.94-12.30 6.37 (57)
BG-T180-male	6	Chr9	T2DSL21*	10.77	10.20-11.18 0.97 (6)	7.16-13.55 6.39 (58)	6.38-14.23 7.85 (69)
BG-T180-male	6	Chr9	T2DSL22*	6.01	5.49-6.61 1.11 (7)	2.98-9.33 6.35 (84)	2.23-10.34 8.11 (88)
AUC0-180- male	6	Chr9	T2DSL24* *	9.09	8.83-9.31 0.48 (5)	7.48-10.52 3.04 (36)	6.77-11.48 4.71 (49)
AUC30-60- male	6	Chr9	T2DSL32* *	9.09	8.94-9.25 0.31 (4)	7.84-10.25 2.40 (21)	7.41-11.47 4.06 (42)
AUC60-120- male	6	Chr9	T2DSL33* *	9.09	8.87-9.30 0.43 (5)	7.56-10.63 3.07 (35)	6.99-11.85 4.86 (49)
AUC120-180- male	6	Chr9	T2DSL36* *	11.25	10.89-11.54 0.65 (4)	8.92-13.53 4.62 (23)	7.83-14.28 6.45 (48)
AUC120-180- male	7	Chr9	T2DSL37* *	51.12	50.64-51.42 0.78 (22)	48.92-52.72 3.79 (67)	48.11-54.09 5.98 (104)
Fasting Glucose (BG-T0)- female	7	Chr9	T2DSL43*	44.39	44.03-44.57 0.55 (38)	42.70-45.76 3.06 (93)	42.13-46.37 4.24 (126)
AUC0-180- male	7	Chr9	T2DSL25* *	51.05	50.81-51.18 0.37 (10)	50.16-51.80 1.64 (41)	49.71-52.16 2.44 (51)

BG - T180- overall	8	Chr11	T2DSL6*	97.16	96.84-97.45 0.61 (31)	95.60-98.62 3.01 (146)	94.96-99.60 4.46 (221)
AUC 120-180- overall	8	Chr11	T2DSL11*	97.08	96.84-97.33 0.48 (29)	95.99-98.25 2.26 (110)	95.44-99.06 3.62 (176)
BG-T60-male	8	Chr11	T2DSL14*	95.92	95.74-96.05 0.31 (17)	95.23-96.53 1.30 (59)	94.98-96.84 1.87 (78)
BG-T120-male	8	Chr11	T2DSL15*	96.48	96.30-96.67 0.37 (13)	95.68-97.52 1.84 (89)	95.21-98.00 2.79 (127)
BG-T180-male	8	Chr11	T2DSL23*	97.84	97.44-98.09 0.64 (36)	96.22-99.16 2.93 (144)	95.72-100.04 4.32 (256)
AUC0-180- male	8	Chr11	T2DSL26* *	96.43	96.22-96.60 0.38 (20)	95.62-97.12 1.50 (78)	95.23-97.47 2.24 (98)
AUC0-120- male	8	Chr11	T2DSL29* *	96.48	96.30-96.64 0.34 (13)	95.95-97.15 1.21 (64)	95.68-97.52 1.83 (89)
AUC120-180- male	8	Chr11	T2DSL38* *	96.48	96.24-96.68 0.45 (21)	95.39-97.33 1.94 (90)	94.91-97.84 2.94 (136)
AUC120-180- male	9	Chr14	T2DSL39* *	79.66	79.36-80.00 0.64 (18)	78.35-81.25 2.91 (39)	77.98-82.24 4.26 (50)
BG - T180- male	9	Chr14	T2DSL19*	79.64	79.38-80.05 0.67 (17)	78.40-81.74 3.34 (41)	77.98-82.70 4.71 (52)
BG - T180- overall	9	Chr14	T2DSL4**	79.26	79.05-79.53 0.48 (16)	78.30-80.68 2.38 (40)	77.95-81.22 3.27 (46)
BG - T180- overall	10	Chr14	T2DSL5**	86.64	86.35-87.13 0.78 (2)	84.62-89.08 4.46 (16)	83.94-89.71 5.76 (21)
BG-T180-male	10	Chr14	T2DSL18* *	86.67	86.16-87.26 1.10 (5)	84.27-89.73 5.46 (21)	83.75-91.22 7.47 (28)
BG-T120-male	11	Chr18	T2DSL17* *	12.26	11.54-12.71	8.19-14.28	6.67-15.70

					1.18 (22)	6.09 (94)	9.03 (134)
AUC0-180- male	11	Chr18	T2DSL28*	12.26	12.01-12.50 0.50 (12)	10.80-13.30 2.50 (41)	9.96-13.71 3.75 (66)
AUC60-120- male	11	Chr18	T2DSL35*	12.26	11.94-12.53 0.59 (12)	10.45-13.38 2.92 (55)	9.08-13.90 4.82 (86)
AUC120-180- male	11	Chr18	T2DSL40*	12.26	12.08-12.45 0.37 (10)	11.34-12.99 1.65 (30)	10.84-13.31 2.47 (49)

Figure 1A.

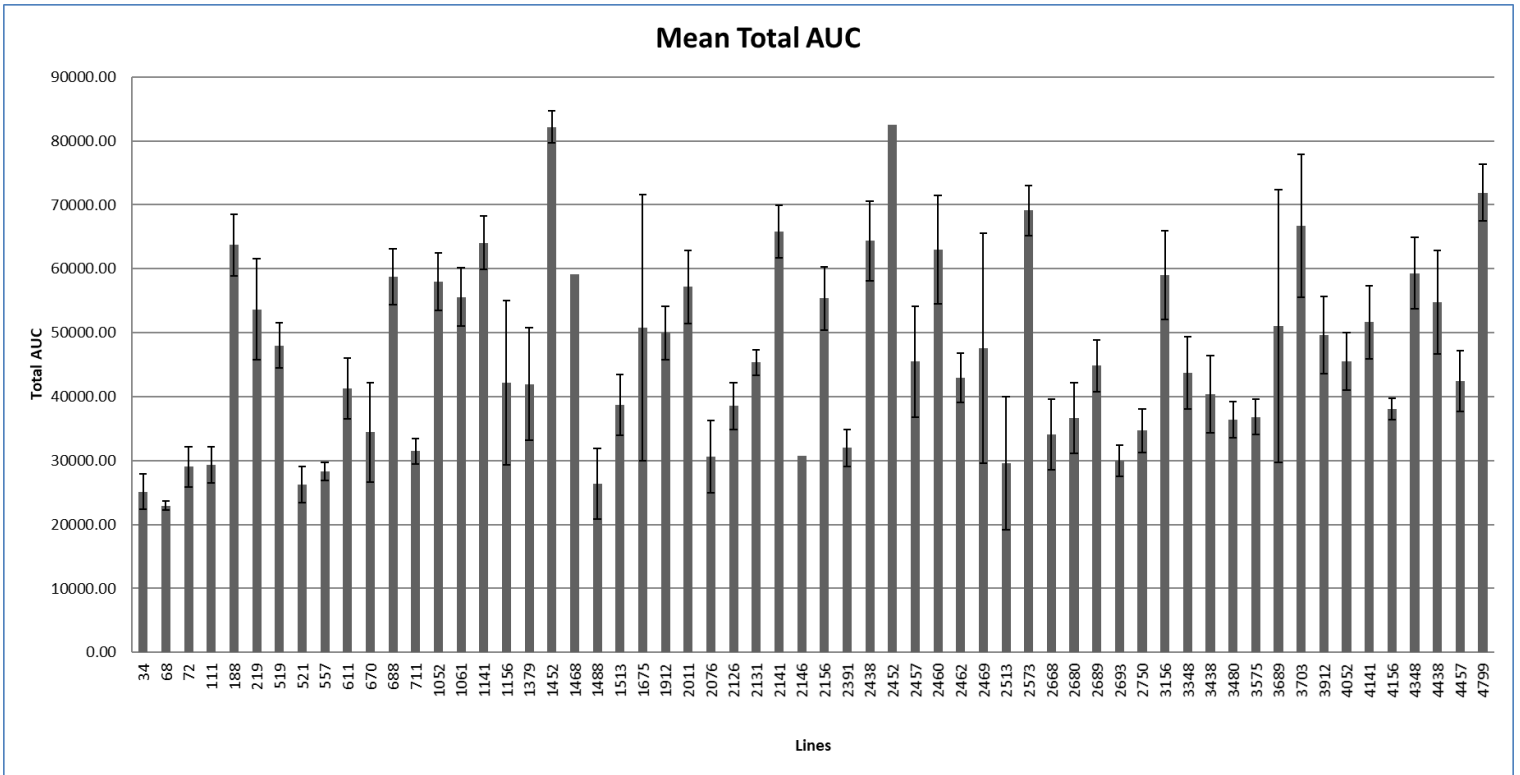


Figure 1B.

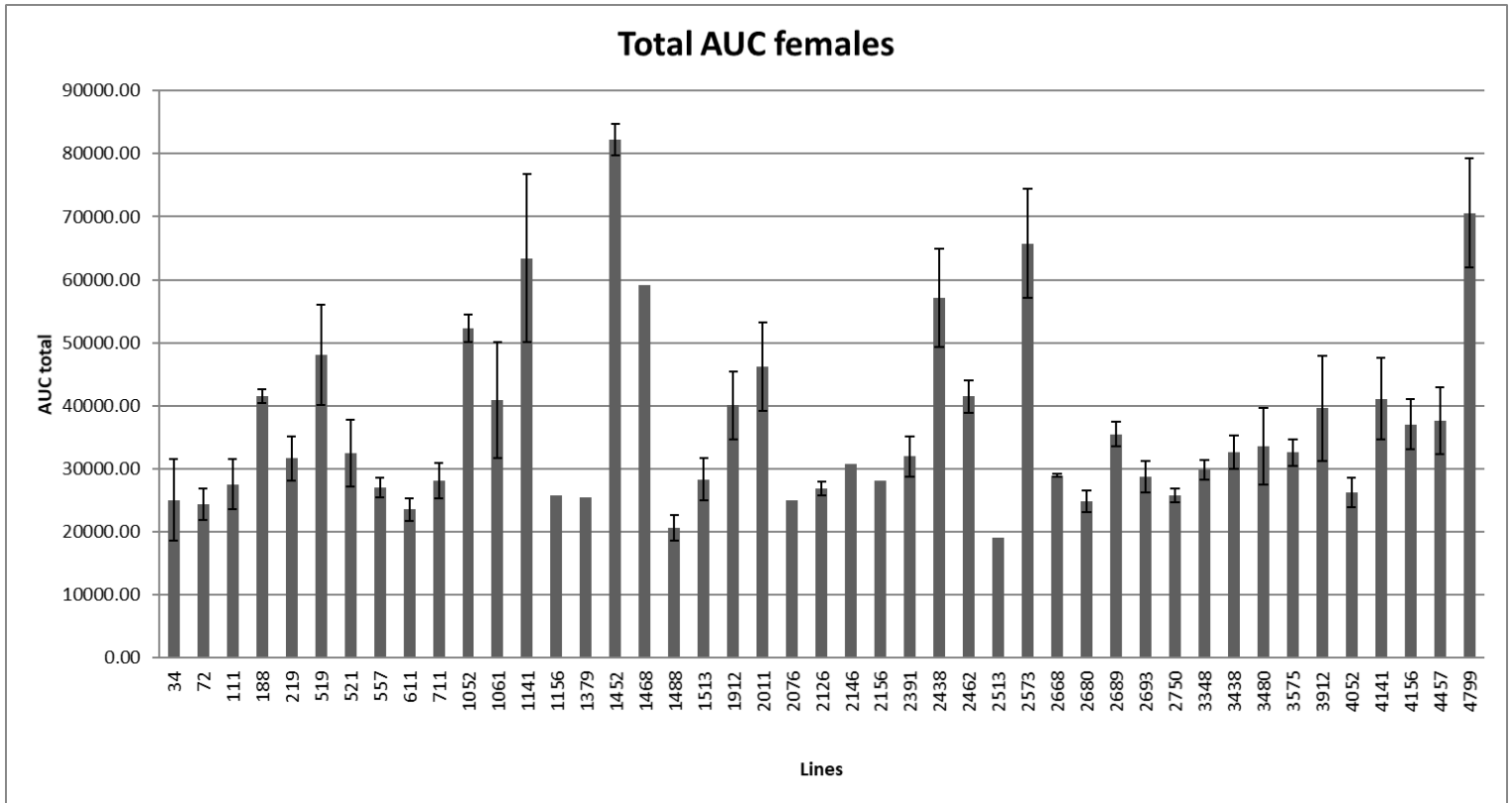


Figure 1C.

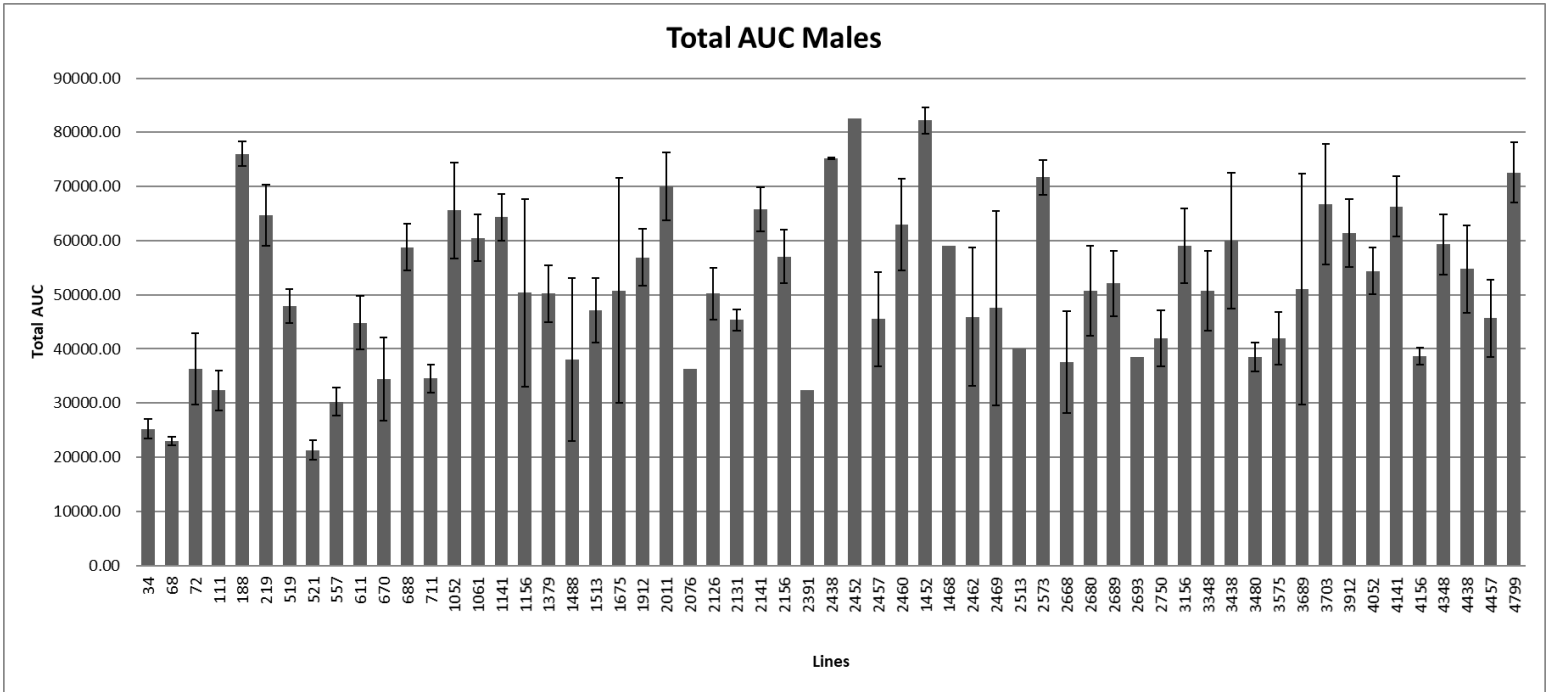


Figure 1D.

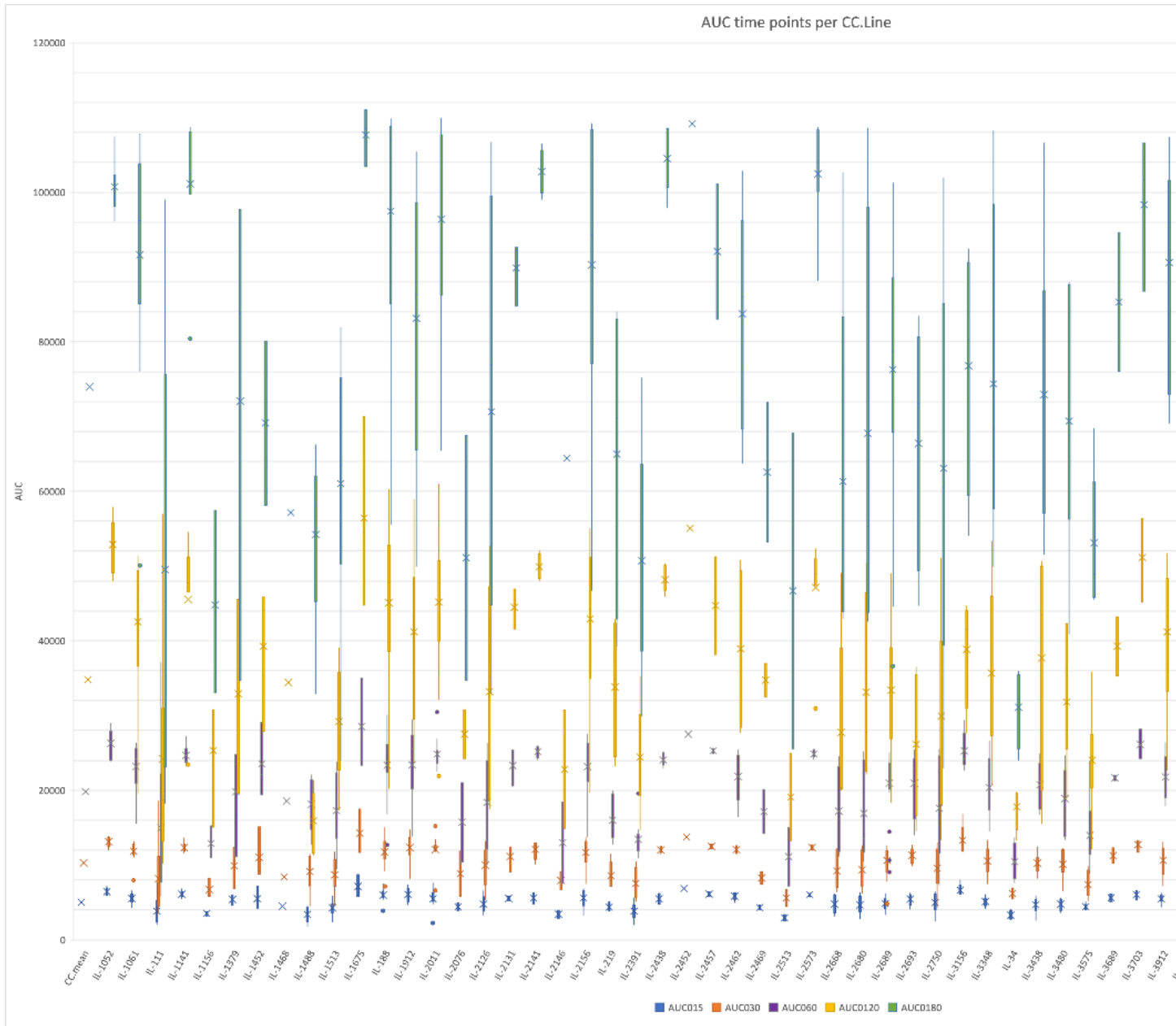


Figure 2A. Overall population

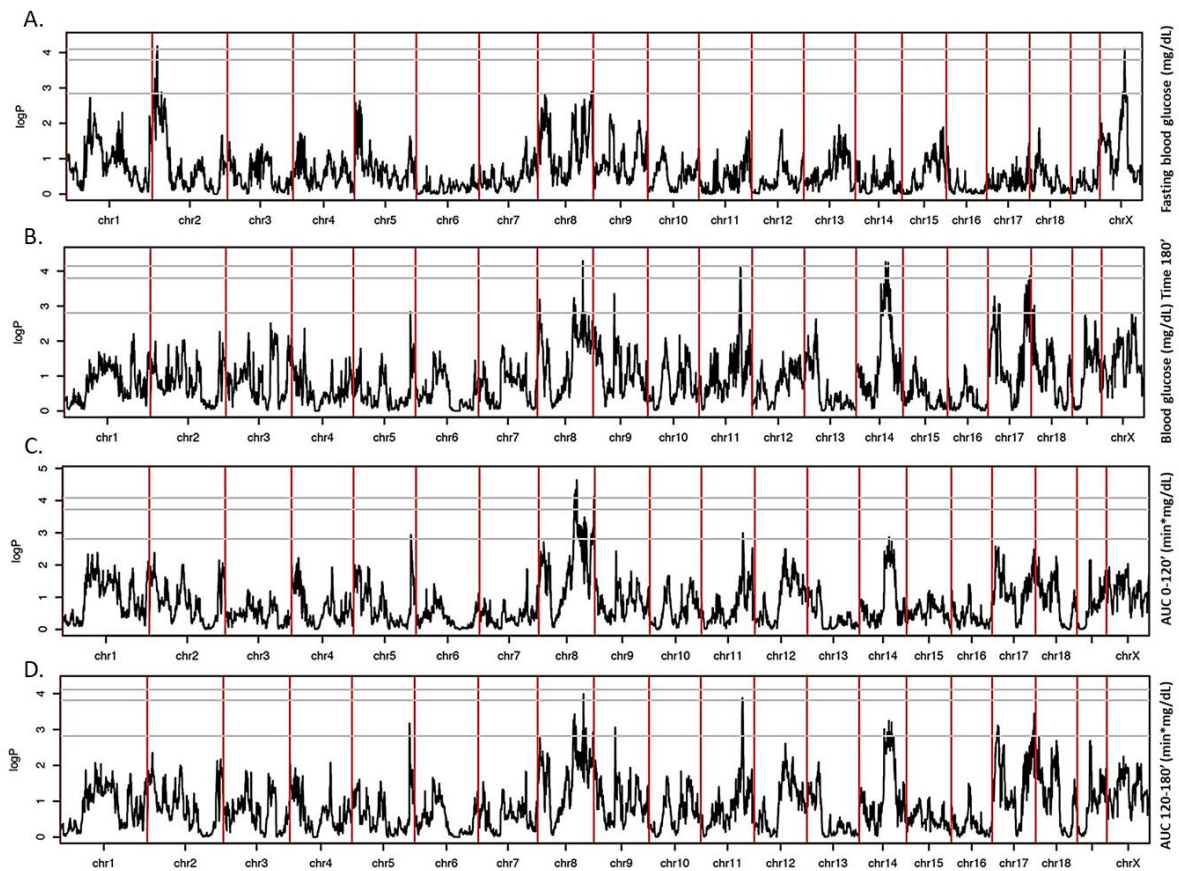


Figure 2B. Males only

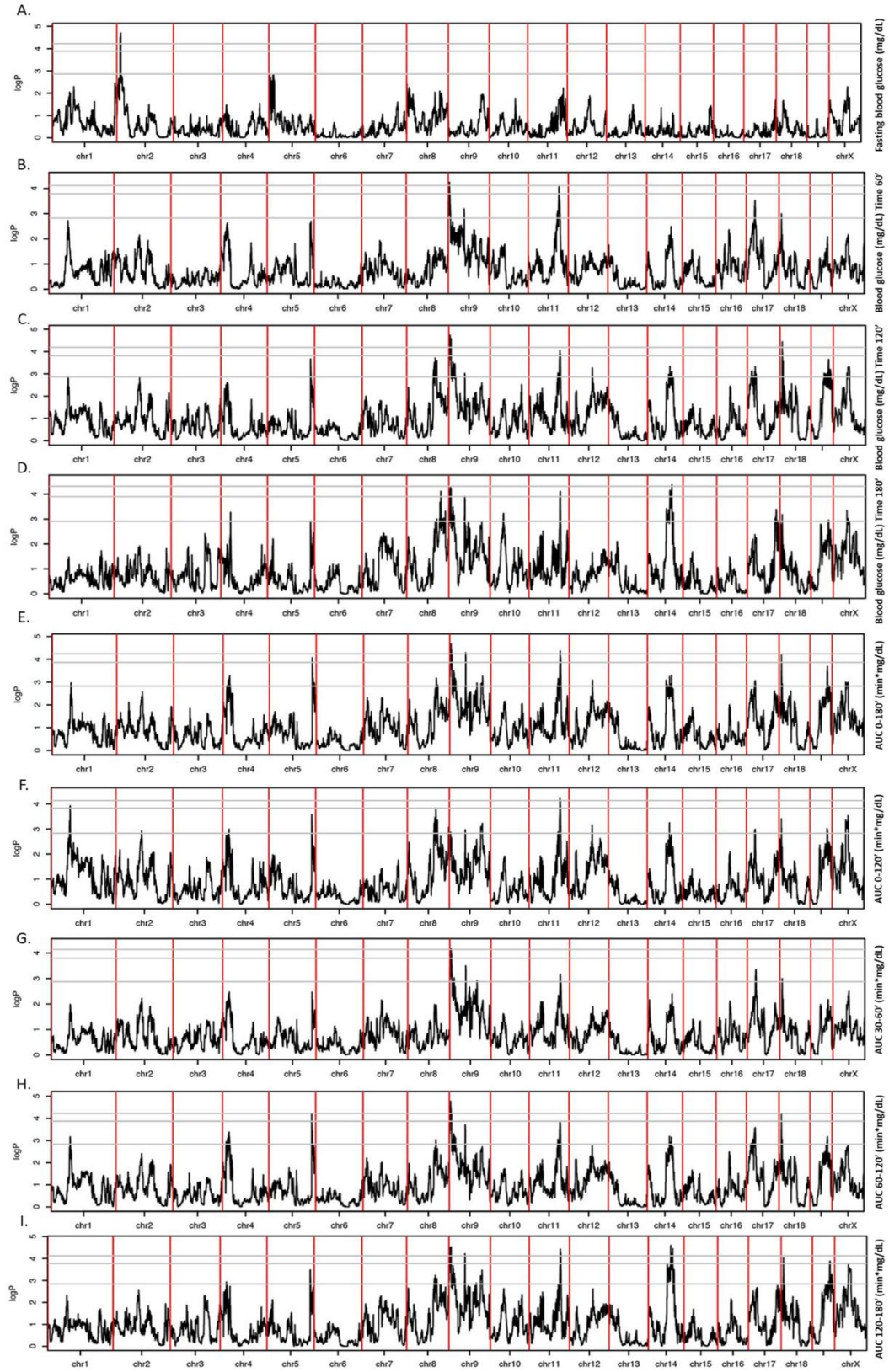


Figure 2C. Females only

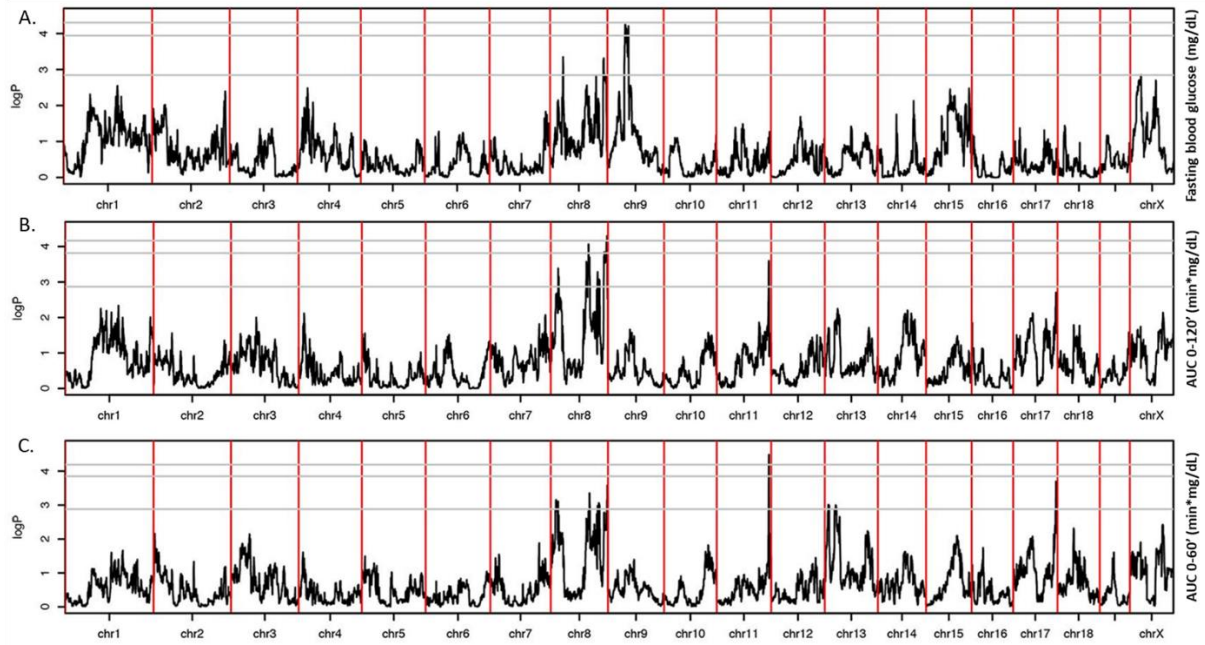


Figure 3A. Overall population

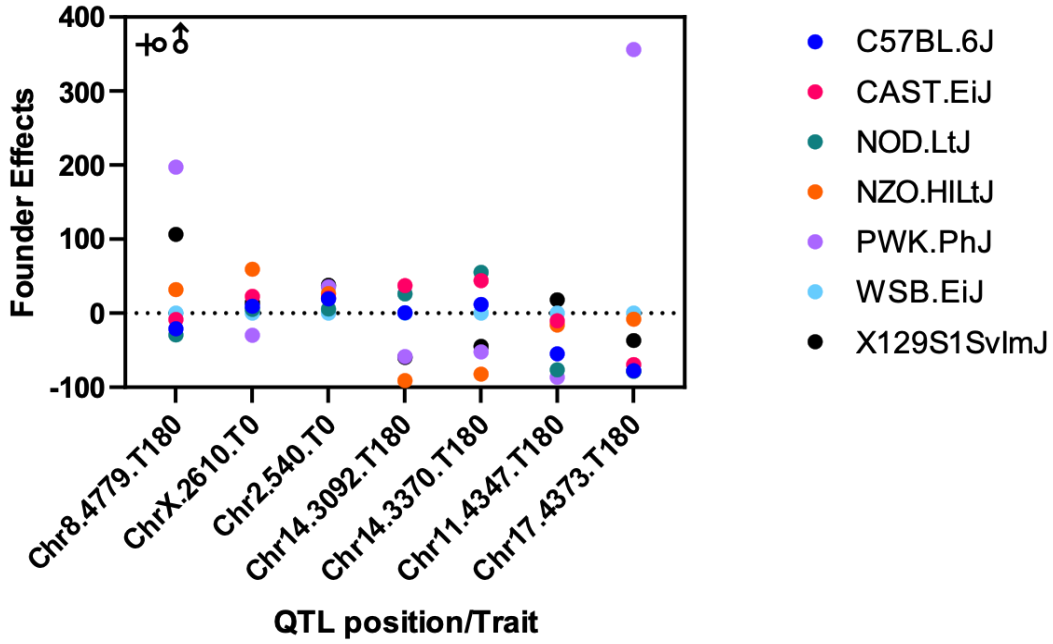


Figure 3B. Overall population

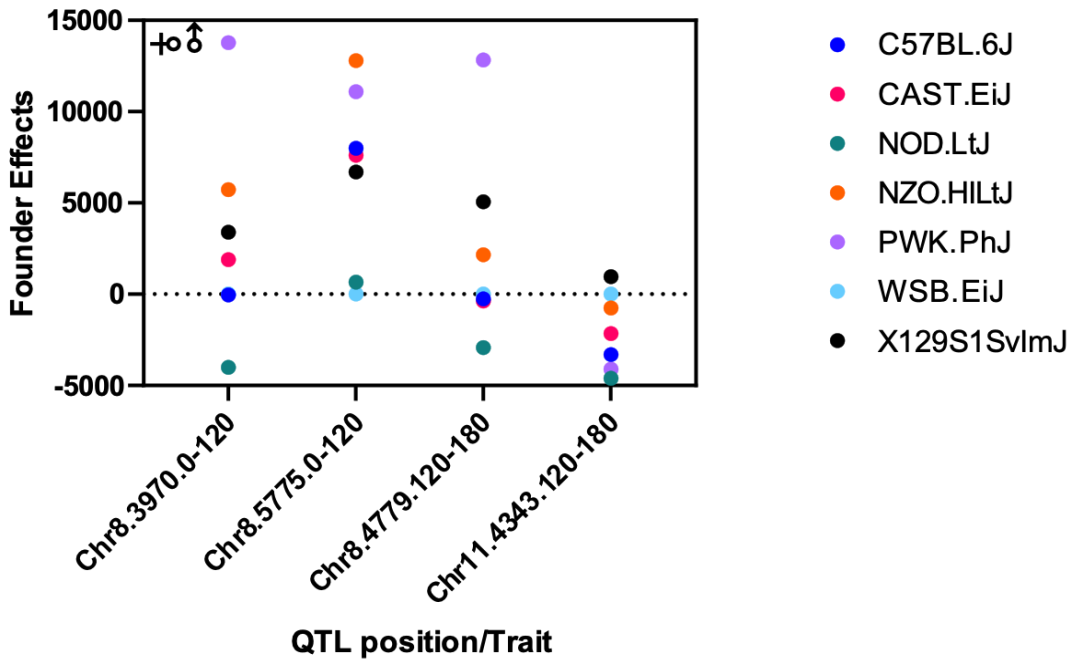


Figure 4A. Males Only

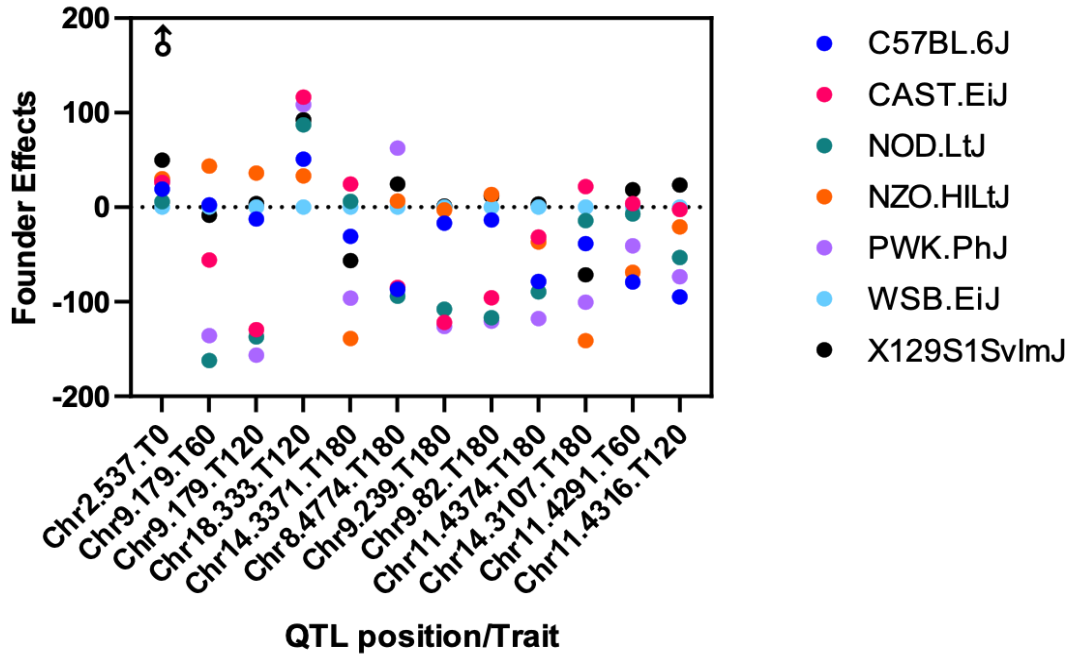


Figure 4B. Males only

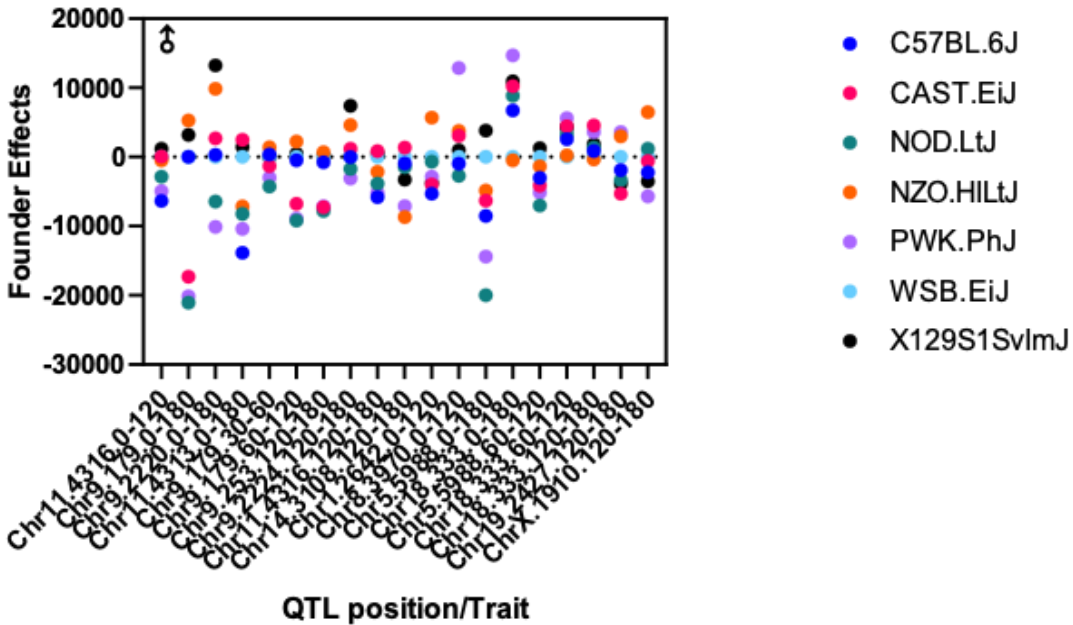


Figure 5A. Females Only

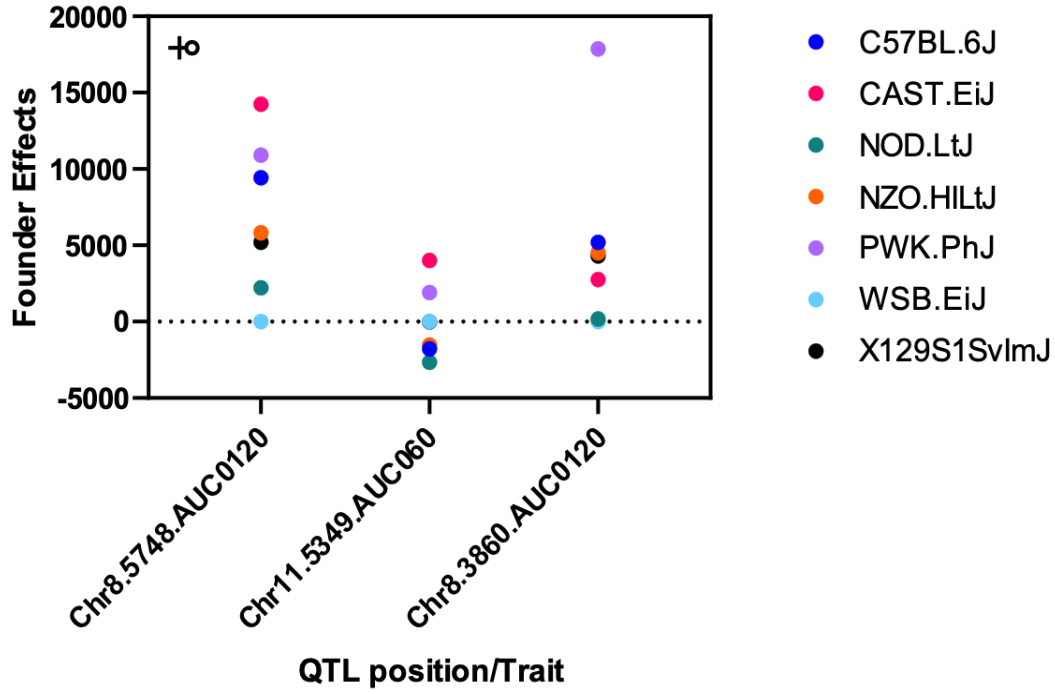


Figure 5B. Females only

